Copy 1

ARR No. L6A05b

NATIONAL ADVISORY COMMITTEE FOR AERONAUTICS

WARTIME REPORT

ORIGINALLY ISSUED

February 1946 as
Advance Restricted Report L6A05b

DETERMINATION OF INDUCED VELOCITY IN FRONT OF AN INCLINED PROPELLER BY A MAGNETIC-ANALOGY METHOD

By Clifford S. Gardner and James A. LaHatte, Jr.

Langley Memorial Aeronautical Laboratory
Langley Field, Va.

NACA

WASHINGTON

NACA ARR No. L6A05b

NATIONAL ADVISORY COMMITTEE FOR AERONAUTICS

ADVANCE RESTRICTED REPORT

DETERMINATION OF INDUCED VELOCITY IN FRONT OF AN INCLINED PROPELLER BY A MAGNETIC-ANALOGY METHOD

By Clifford S. Gardner and James A. LaHatte, Jr.

SUMMARY

The horizontal and vertical components of the induced velocity in front of an inclined propeller in a horizontal stream were obtained by a magnetic-analogy method. The problem was formulated in terms of the linear theory of the acceleration potential of an incompressible nonviscous fluid. The propeller was assumed to be an actuator disk. The horizontal component of the induced velocity was found by a numerical calculation. Numerical calculation of the vertical component, however, was not practicable; therefore the vertical component was obtained from electrical measurements by use of the analogy between the acceleration potential of an incompressible nonviscous fluid and the potential of a magnetic field.

An alternative formulation of the problem in terms of the trailing-vortex sheet is shown to be equivalent to the acceleration-potential formulation if the thrust coefficient is assumed so small that the slipstream is not deflected and undergoes no contraction. From the results presented, induced velocities of greater accuracy are shown to be obtainable from a modification of the vortex theory based on the assumption of a constant finite downwash angle of the slipstream.

INTRODUCTION

The recent development of airplane designs with pusher-propeller installations has occasioned several inquiries regarding the nature of the flow in front of an inclined propeller and the corresponding aerodynamic effects on the wing. Because of the difficulty of the calculations, little effort has heretofore been made to

compute the flow. Some experimental work, however, has been done in connection with the problem of the lift increment on the wing (for example, references 1 and 2). Further development of the theory is considered desirable to serve as a basis for correlation of these and similar data.

The purpose of the present paper is to give detailed theoretical data on the induced velocities in front of an inclined propeller. Only the components important to the problem have been obtained; namely, the component parallel to the free-stream direction and the component normal to the free stream and in a vertical plane, which will be designated horizontal and vertical components, respectively. The determination of these components is based on the linear theory of the acceleration potential of an incompressible nonviscous fluid, and the propeller is assumed to be an actuator disk. Because the theory is valid only for small perturbations, the results, which are presented in dimensionless form independent of the thrust coefficient, are valid only if used for propellers operating at low thrust coefficients.

The horizontal component of the induced velocity was determined by numerical computation. The computation of this component was practicable because of certain simplifications due to symmetry. Numerical calculation of the vertical component, however, is excessively laborious and time-consuming; consequently, the vertical component was obtained from electrical measurements by use of the analogy between the acceleration potential of an incompressible nonviscous fluid and the potential of a magnetic field.

An alternative formulation of the problem in terms of the trailing-vortex sheet is shown to be equivalent to the acceleration-potential formulation if the thrust coefficient is assumed so small that the slipstream is not deflected and undergoes no contraction. From the results presented, induced velocities of greater accuracy are shown to be obtainable from a modification of the vortex theory based on the assumption of a constant finite downwash angle of the slipstream.

SYMBOLS

p	local static pressure
p_1	static pressure at downstream face of propeller disk
ρ	air density
t	time
x, y, z	rectangular coordinates (fig. 1)
V	free-stream velocity
u, v, w	components of perturbation velocity in X-, Y-, and Z-directions, respectively
I	electric current, cgs electromagnetic units
R	radius of propeller
D	diameter of propeller
T	thrust of propeller
T_c	thrust coefficient $\left(\frac{T}{\rho V^2 D^2}\right)$
u', v', w'	dimensionless velocities $\left(\frac{u}{VT_c}, \frac{v}{VT_c}, \frac{w}{VT_c}\right.$, respectively$\left.\right)$
p'	dimensionless pressure $\left(\frac{p}{\rho V^2 T_c}\right)$
x', y', z'	dimensionless coordinates (x/R, y/R, z/R, respectively)
ϕ	magnetic scalar potential, cgs electromagnetic units
H_x, H_y, H_z	components of magnetic-field strength, cgs electromagnetic units
E	experimentally measured voltage, volts

K ratio of w' to analogous measured voltage E

α angle of inclination of propeller disk to Z-axis, degrees

ϵ assumed constant downwash angle of slipstream, radians

M mass rate of flow across propeller disk

Subscripts:

2 in ultimate wake

1 at downstream face of propeller disk

THEORY OF THE METHOD

Linear theory of the acceleration potential.- The Euler equations for the flow of an incompressible nonviscous fluid may be written in the following form:

$$\left.\begin{aligned} \rho \frac{D(V + u)}{Dt} &= -\frac{\partial p}{\partial x} \\ \rho \frac{Dv}{Dt} &= -\frac{\partial p}{\partial y} \\ \rho \frac{Dw}{Dt} &= -\frac{\partial p}{\partial z} \end{aligned}\right\} \qquad (1)$$

These equations are in general nonlinear in the velocities. The equations may be made linear if the components of the perturbation velocity are assumed to be small compared with the free-stream velocity. (See reference 3.) If this assumption is valid and if terms of the second order are neglected,

$$\left.\begin{aligned} \frac{D(V + u)}{Dt} = \frac{Du}{Dt} &= V \frac{\partial u}{\partial x} \\ \frac{Dv}{Dt} &= V \frac{\partial v}{\partial x} \\ \frac{Dw}{Dt} &= V \frac{\partial w}{\partial x} \end{aligned}\right\} \qquad (2)$$

By virtue of equations (2), equations (1) become

$$\rho V \frac{\partial u}{\partial x} = -\frac{\partial p}{\partial x} \tag{3a}$$

$$\rho V \frac{\partial v}{\partial x} = -\frac{\partial p}{\partial y} \tag{3b}$$

$$\rho V \frac{\partial w}{\partial x} = -\frac{\partial p}{\partial z} \tag{3c}$$

If equations (3) are differentiated successively with respect to x, y, and z and are added, the result is

$$-\nabla^2 p = \rho V \frac{\partial}{\partial x}\left(\frac{\partial u}{\partial x} + \frac{\partial v}{\partial y} + \frac{\partial w}{\partial z}\right) = 0 \tag{4}$$

Magnetic analogy.- Since by equation (4) p satisfies Laplace's equation, and since the scalar potential of a magnetic field also satisfies Laplace's equation, it follows that for similar boundary conditions p is directly analogous to the scalar potential of a magnetic field. This fact is the theoretical basis of the magnetic analogy of the present paper.

For low thrust coefficients the three boundary conditions for the pressure p in the problem of the actuator disk are:

(1) The pressure has some constant value $-p_1$ uniformly over the upstream face of the disk and a value p_1 uniformly over the downstream face.

(2) The pressure has no singularities other than the jump discontinuity at the disk.

(3) At great distances from the disk, the pressure is uniform and without loss of generality may be assumed to be zero.

For the magnetic potential the first condition is satisfied by using as the source of the magnetic field a circular wire loop carrying a current. The use of this

current-carrying loop actually ensures the appropriate behavior of the magnetic field at the disk since the magnetic potential of such a loop has the value $-2\pi I$ uniformly over one face of the loop and the value $2\pi I$ over the other face - if cgs electromagnetic units are used (reference 4). The second condition is satisfied if no other magnetic fields and no magnetic materials are in the neighborhood of the loop. The third condition is satisfied automatically, since the magnetic potential of the loop approaches zero at great distances from the loop.

Basis of determination of horizontal velocity.- If equation (3a) is integrated with respect to x, the result is

$$\rho V u = -p \tag{5}$$

Inasmuch as the dimensionless velocity u' and the dimensionless pressure p' are defined by

$$u' = \frac{u}{VT_c}$$

and

$$p' = \frac{p}{\rho V^2 T_c}$$

equation (5) becomes

$$u' = -p' \tag{6}$$

The value of the dimensionless pressure p' at the downstream face of the disk is

$$p_1' = \frac{p_1}{\rho V^2 T_c}$$

$$= \frac{p_1}{\rho V^2 \left[\frac{\left(\frac{\pi}{4}D^2\right)\left(2p_1\right)}{\rho V^2 \pi^2}\right]}$$

$$= \frac{2}{\pi} \tag{7}$$

Since this boundary value is a universal numerical constant, the values of the dimensionless velocities throughout space, which are determined by the boundary values of p', are also universal numerical constants. By means of the dimensionless coefficients u', v', w', and p', therefore, the problem is stated in a nondimensional form that is independent of all relevant variables such as the disk radius, density, thrust, and free-stream velocity.

In accordance with the magnetic analogy, the magnetic potential is directly analogous to the pressure p'; that is,

$$p' = k\phi \tag{8}$$

where ϕ is the magnetic potential measured at a point of which the dimensionless coordinates x', y', and z' are the same as the dimensionless coordinates of the point where p' is measured, and where k is some constant of proportionality that depends on the dimensions of the electromagnetic system. The value of p' and, hence, u' was thus obtained by calculating ϕ and multiplying by the constant k_1 which may be determined by comparing the value of p' at the disk, which by equation (7) is $2/\pi$, with the value of ϕ at the disk, which is $2\pi I$. The calculation of ϕ was effected by numerical integration of a formula given by Smythe (reference 5) for the magnetic field of a circular loop.

The potential ϕ and, consequently, the horizontal velocity u' at any point depend only on the position of this point relative to the disk; thus, the results for u' at positions given in terms of coordinates fixed in the disk are the same for all angles of inclination. Because of rotational symmetry, moreover, the values of u' at corresponding points in any two planes through the axis of the disk are the same. It was thus necessary to calculate u' over only one axial plane.

The linear theory of the present paper gives values of $u' = \frac{u}{VT_c}$ that are valid for low thrust coefficients; that is, the results for u' are essentially the derivatives of u/V with respect to T_c at $T_c = 0$. The momentum theory of the propeller (reference 6) gives the inflow velocity at the disk as

$$u = \frac{V}{2}\left(\sqrt{1 + \frac{8T_c}{\pi}} - 1\right)$$

The value of u' at the disk should therefore be

$$u' = \left(\frac{d\frac{u}{V}}{dT_c}\right)_{T_c=0} = \frac{2}{\pi}$$

a value that checks exactly with the value given by the linear theory of the present paper (equations (6) and (7)).

Basis of determination of vertical velocity.- If equation (3c) is integrated with respect to x, from $-\infty$ to x, the result is

$$\rho V w = -\int_{-\infty}^{x} \frac{\partial p}{\partial z} dx \tag{9}$$

If equation (9) is divided by $\rho V^2 T_c$ and if dimensionless coordinates are introduced, the result is

$$w' = -\int_{-\infty}^{x'} \frac{\partial p'}{\partial z'} dx' \tag{10}$$

In accordance with the magnetic analogy, if equation (8) is used, equation (10) becomes

$$w' = -\int_{-\infty}^{x'} k \frac{\partial \phi}{\partial z'} dx'$$

$$= k \int_{-\infty}^{x} -\frac{\partial \phi}{\partial z} dx \tag{11}$$

But since ϕ is the potential of a magnetic field,

$$-\frac{\partial \phi}{\partial z} = H_z$$

where H_z is the z-component of the magnetic-field strength. Equation (11) now becomes

$$w' = k \int_{-\infty}^{x} H_z \, dx \qquad (12)$$

In order to find the value of w' at a point (x', y', z') it is therefore sufficient to measure the integral of H_z along a path parallel to the X-axis, extending from minus infinity to the point (x, y, z).

An alternating magnetic field in air induces in a coil of wire a voltage proportional to the total flux linking the coil, which in turn is proportional to the integral over the face of the coil of the normal component of the magnetic-field strength. The voltage induced in a long narrow search coil is proportional to the surface integral of the normal field over the area of this coil; since the coil is narrow and, consequently, the field strength is almost constant across the width of the coil, this surface integral is proportional to the line integral along the length of the coil. The line integral in equation (12), therefore, is proportional to the voltage induced in a long narrow search coil, the plane of which is perpendicular to the Z-axis, which extends parallel to the X-axis from the point $(-\infty, y, z)$ to the point (x, y, z), as shown in figure 2. Since the magnetic field dies out rapidly with distance, a search coil of practical length actually suffices to obtain accurately enough the infinite integral.

Thus the following equation holds:

$$w' = KE \qquad (13)$$

where E is a measured voltage proportional to the voltage induced in the search coil and K is a constant of proportionality to be determined by calibration.

APPARATUS AND METHODS

Field coil.- A field coil of 64 turns of Brown and Sharpe No. 18 copper wire wound on a circular wooden form was used to simulate the actuator disk. The mean radius of the coil was 12 inches and the cross section was a square 0.875 inch by 0.875 inch. The coil was supported by pivots about its horizontal diameter in such a way that its angle of inclination to the Z-axis could be varied and the support could be moved up and down. The arrangement is shown in figure 2.

Search coil.- As previously explained, a long narrow search coil was used to perform the integration of the magnetic-field strength indicated in equation (12). The search coil was made up of 110 turns of Brown and Sharpe No. 40 copper wire wound lengthwise on a glass rod 72 inches by 0.225 inch by 1.2 inches. The coil rested on Lucite supports at the two ends. The supports were scribed with cross-hair lines to aid in setting the position of the coil and were supplied with leveling screws so that the face of the coil could be turned exactly 90° to the flux being measured. The voltage developed in the search coil was fed through a filter eliminating 60-cycle pickup to an electronic voltmeter by which the voltage was measured.

Power supply.- Current was supplied to the field coil from a motor-generator set delivering 5.0 amperes at 390 cycles per second. The Ward-Leonard speed control system was used so that the frequency and output voltage could be adjusted by rheostats. The output voltage was continuously adjusted to maintain through the field coil a constant current of 5.0 amperes, as measured on a standard high-frequency ammeter. The output of the generator was connected in parallel with the input of a cathode-ray oscilloscope, and a 60-cycle line voltage was connected across the sweep circuit. The resulting Lissajous pattern was held stationary by continuous adjustment of the frequency control rheostat; thus the frequency of the current was maintained constant at 390 cycles per second. The arrangement is shown in figure 3.

Test procedure.- In order to measure the integral in equation (12) at the point (x, y, z) when the disk

was inclined to the Z-axis by an angle α, the field coil was set so that its center was a distance z below a horizontal table; then it was set at the angle α with a protractor and the search coil was placed on the table parallel to the X-axis with one end at the point (x, y, z) and the other end away from the field coil. The arrangement is shown in figure 2. For each setting of α and z, readings of the voltage were made at the 170 vertices of a rectangular grid 64 inches by 40 inches that was made up of lines parallel to the X-axis and the Y-axis spaced at intervals of 4 inches. The arrangement is shown in figure 1.

Zero height adjustment.- In order to locate the height of the field coil corresponding to a value of $z = 0$, α was set at 0° and the height of the field coil was then adjusted for zero voltage in the search coil. The voltage in the search coil is zero when α and z are zero, so that the search coil is on a plane through the axis of the field coil, since the component of the magnetic field normal to such a plane is zero.

Leveling adjustment for the search coil.- The component H_z of the magnetic field is symmetric about the XZ-plane for all values of α; consequently if the search coil actually measures the component H_z of the magnetic field, the voltage readings should be the same for two positions of the search coil in which the values of x and z are the same and in which the values of y have equal magnitudes but opposite signs. If, however, the search coil is not level so that the component H_y also contributes to the induced voltage, the voltage readings will not be the same at symmetric points since H_y has opposite signs at symmetric points. When the component H_y is strong, the error in the voltage reading may be large if the search coil is not level; hence at each setting of α and z the coil was leveled by adjusting the leveling screws until the readings were the same for a pair of symmetric positions. Because of some unevenness of the table top on which the search coil rested, the readings were not exactly the same for other pairs of symmetric positions; hence average values were used for the data at other positions.

Calibration of the magnetic analogy apparatus.- In order to calculate w' from the voltage readings by use

of equation (13) determination of the value of the constant K was necessary. This value was obtained by calibrating the apparatus; that is, by comparing values of E measured at a series of calibration points with values of w' calculated for those points. The values of w' were calculated from equation (12) by use of an electromagnetic formula (reference 5). The method is similar to the method previously discussed by which the horizontal velocity u' was calculated.

The values of w' were calculated for values of $\alpha = 90^\circ$ and $z = 0$ at a series of points along the X-axis. A comparison of calculated values of w' and measured values of E is given in table I to show how the calibration constant K was obtained.

Accuracy.- In order to estimate the accuracy of the experiment, values of w' were computed at several points for a value of $\alpha = 0^\circ$ and were compared with the corresponding experimental values. The experimental values were found to be low, some by as much as 8 percent. This inaccuracy in the data can be attributed to errors in the measurement of distances and angles and to the fact that the search coil used was of finite length. The error due to the finite length of the search coil could be calculated by means of the assumption that at great distances from the field coil the magnetic field could be approximated by the field of a magnetic dipole. This error was found to amount to less than 5 percent at great distances from the field coil, where the magnetic field falls off slowly with distance. In general, about half of the error may be attributed to the finite length of the search coil and the other half, to inaccuracies in measuring distances and angles.

The error of the calibration readings (table I) may be seen to be less than the 8 percent error mentioned previously. This greater precision is probably due to the fact that for values of $\alpha = 90^\circ$ and $z = 0$ the voltage reading is insensitive to small errors in the alinement of the field and search coils because the magnetic field is symmetric about the origin and is a maximum relative to both α and z.

RESULTS

The horizontal velocity field of the actuator disk is presented in figure 4 as a map of contours of constant dimensionless horizontal velocity u' in a plane through the axis of symmetry of the disk. The horizontal velocity at any point for any value of α is then the same as the horizontal velocity at the corresponding point that is in this plane of symmetry and has the same position in terms of coordinates fixed in the actuator disk.

The vertical velocity field of the actuator disk is presented in figures 5 to 9 as a series of maps of contours of constant dimensionless vertical velocity w' for five different values of α at nine vertical sections that are parallel to the free stream and spaced at intervals of 1/3 radius from values of $y = 0$ to $y = 2\frac{2}{3}$ radii.

In order to plot each contour map, averages of the voltage readings on the two sides of the XZ-plane were used. On each section the contours of constant velocity are drawn throughout a rectangular area extending horizontally 3 radii upstream from the actuator disk and vertically 1 radius above and below the center of the disk. The nine sections on which contour maps are drawn are labeled a to i from the plane of symmetry outwards, as shown in figure 1.

VORTEX TREATMENT OF ACTUATOR-DISK PROBLEM

Equivalence at low thrust coefficients of vortex and acceleration-potential formulations of actuator-disk problem.- It is shown in reference 7 that there is associated with an actuator disk at low thrust coefficient a cylindrical sheet of circular vortex rings, which leave the disk and travel downstream in the free-stream direction. This vortex pattern is approximated by a propeller operating at low thrust coefficient and rotational speeds high in comparison with the free-stream velocity and having blades along which the bound vortex strength is uniform. Because the bound vortex strength is uniform, trailing vortices leave the blades only at the tips and at the center of the propeller. The tip vortices travel downstream in helical paths and the vortices from the propeller center travel downstream in a straight line.

At any instant the density of the bound vortices and of the trailing vortices from the propeller center is negligible compared with the density of the helical vortices, since the density of these tip vortices is proportional to the high speed of the blade tips. The velocity field of the propeller is therefore the induced velocity field of the infinite cylindrical vortex sheet shed from the blade tips. Since the rotational velocity is high, the pitch of a helical vortex is small and the sheet can therefore be considered to consist of an infinite continuous row of circular vortex lines.

It may also be shown that the induced velocity field of a propeller operating at low rotational speed and low thrust coefficient and having an infinite number of blades along which the bound vortex strength is uniform is the same outside the slipstream as the velocity field of an actuator disk. The vortex pattern of such a propeller may be considered to consist of a system of vortex rings to which must be added another vortex system composed of the radial bound vortices together with straight trailing vortices from the propeller center and from the blade tips. The induced velocity field of the system of rings is the same as that of an actuator disk. The induced velocity field of the remaining vortex system, however, may be shown to be zero outside the slipstream. The rotational induced velocity is zero because of rotational symmetry and the fact that the total circulation around a closed path exterior to the slipstream is zero (since the total included vorticity is zero). The radial and axial components are zero, since only the radial bound vortex elements in the plane of the disk could contribute to such components and the contribution of these elements vanishes because of symmetry.

The velocity field of an actuator disk may be calculated by integrating the effect of the infinite row of circular vortex lines. Since the velocity induced by a vortex line is directly analogous to the magnetic field of a current filament, the induced velocity of the infinite vortex sheet is analogous to the integral of the magnetic field of an infinite row of circular current filaments. This integral, in which the point at which the field is evaluated is fixed and the position of the source is variable, evidently has the same value as a related integral of the magnetic field at a variable point due to a fixed source. The related integral, however, as

has been shown previously, gives the induced velocity according to the acceleration-potential formulation of the problem. Under the assumption of small perturbations, the alternative treatment of the problem of the actuator disk using the trailing vortex sheet, which may be considered to be the treatment in terms of the velocity potential, yields the same results as the treatment in terms of the acceleration potential.

Modification of vortex sheet formulation for high thrust coefficients.- A limitation in the theory as presented thus far is the fact previously noted that the results are valid only at low thrust coefficients. In the acceleration-potential formulation, the source of this limitation occurs in the assumption that the perturbation velocities are small compared with the free-stream velocity; in the trailing vortex formulation, the limitation occurs in the assumptions that the slipstream undergoes no contraction and that it travels downstream in the free-stream direction. The theory of the vortex formulation may be modified to give greater accuracy at high thrust coefficients by assuming that the slipstream is deflected downward from the free stream by a constant finite angle ϵ. The downwash angle in the ultimate wake ϵ_2 may be determined by a simple calculation and may be taken as the value of ϵ. Since, however, the maximum influence is exerted by the trailing vortices just behind the propeller, it might be more accurate to use as the value of ϵ the downwash angle immediately behind the propeller, which is about one-half of ϵ_2. The integration is then performed in the direction of the trailing vortex sheet rather than in the free-stream direction, the direction of the X-axis (fig. 10). If the X-axis and the Z-axis are rotated through an angle ϵ about the Y-axis to form a new set of coordinate axes $(\bar{X}, Y, \bar{Z})$, the integration in the direction of the slipstream is integration along the $\bar{X}$-axis of the field of a coil making an angle $\alpha - 57.3\epsilon$ (in deg) with the $\bar{Z}$ axis. (See fig. 10.) The components of the perturbation velocity parallel to the $\bar{X}$-axis and the $\bar{Z}$-axis can be obtained from the results presented in figures 4 to 9 for the horizontal and vertical perturbation velocities for the angle $\alpha - 57.3\epsilon$. From the $\bar{x}$- and $\bar{z}$-components of the perturbation velocity, the x- and z-components may then be found by a simple calculation.

Calculation of slipstream downwash angle.- The downwash angle ϵ_2 may be calculated by equating the components of the propeller thrust parallel and normal to the free stream to the corresponding components of the rate of change of momentum of the air flow. When the normal thrust-momentum equation is set up, care must be exercised to include the momentum of the flow about the slipstream; that is, the momentum of its virtual mass (references 8 and 9). The normal thrust-momentum equation therefore is

$$\frac{T\alpha}{57.3} = M(V + u_2)\epsilon_2 + MV\epsilon_2 \qquad (14)$$

where M is the mass rate of flow across the propeller disk, and u_2 is the velocity increment in the slipstream in the ultimate wake. The term $M(V + u_2)\epsilon_2$ of equation (14) is the vertical momentum in the slipstream; the term $MV\epsilon_2$ is the vertical momentum of the virtual mass of the slipstream. The thrust is given by the equation

$$T = Mu_2 \qquad (15)$$

Substitution of equation (15) in equation (14) gives

$$57.3\epsilon_2 = \frac{u_2\alpha}{u_2 + 2V} \qquad (16)$$

In order to apply equation (16) the value

$$u_2 = V\left(\sqrt{1 + \frac{8T_c}{\pi}} - 1\right) \qquad (17)$$

derived from the momentum theory of the propeller with no inclination (reference 6) may be used.

In practice, the correction angle ϵ is very small. For example, if $\alpha = 10^\circ$ and $T_c = 0.2$, equation (17) becomes

$$u_2 = V\left(\sqrt{1 + \frac{8 \times 0.2}{\pi}} - 1\right)$$

$$u_2 = 0.228V$$

and, consequently, equation (16) becomes

$$57.3\epsilon_2 = \frac{0.228V \times 10}{0.228V + 2V} \approx 1$$

which gives for ϵ a value of

$$\epsilon = \frac{1}{2}\epsilon_2 = \frac{0.5}{57.3} \text{ radian} \approx 0.5^\circ$$

EFFECT OF PUSHER PROPELLER ON LIFT AND PITCHING MOMENT OF WING

The incremental horizontal and vertical velocities induced by a pusher propeller may be expected to cause an increase in the lift of the wing (reference 1) and a decrease in the pitching moment, inasmuch as these incremental velocities increase toward the trailing edge. The results of the present paper indicate that the induced vertical velocities (figs. 5 to 9) in the region directly ahead of the propeller are small in comparison with the induced horizontal velocities (fig. 4). The effect of the induced vertical flow on the lift and pitching moment of the wing may consequently be expected to be small in comparison with the effect of the induced horizontal flow. Calculation of the magnitudes of the increments of lift and pitching moment due to the presence of the pusher propeller is however considered impracticable, inasmuch as (1) the available lifting surface theories require a prohibitive amount of labor, especially for a flow field as nonuniform as that in front of a propeller, and (2) the changes wrought by the pressure field and velocity field of the propeller in the boundary layer, which cannot be taken into account in the lifting-surface theory, are expected to cause increments in lift and moment comparable with the total increments due to the presence of the pusher propeller (reference 1). It may be concluded, then, that further work both to clarify the physical phenomena and to improve the computational methods will

be required before the effect of the propeller on the wing can be accurately predicted.

Langley Memorial Aeronautical Laboratory
National Advisory Committee for Aeronautics
Langley Field, Va.

REFERENCES

1. Smelt, R., and Smith, F.: Note on Lift Change Due to an Airscrew Mounted behind a Wing. Rep. No. B.A. 1514, British R.A.E., Dec. 1938, and Addendum, Rep. No. B.A. 1514a, April 1939.

2. Thompson, J. S., Smelt, R., Davison, B., and Smith, F.: Comparison of Pusher and Tractor Airscrews Mounted on a Wing. Rep. No. B. A. 1614, British R.A.E., June 1940.

3. Prandtl, L.: Recent Work on Airfoil Theory. NACA TM No. 962, 1940.

4. Page, Leigh, and Adams, Norman Ilsley, Jr.: Principles of Electricity. D. Van Nostrand Co., Inc., 1931, pp. 19, 131-133, 253-257.

5. Smythe, William R.: Static and Dynamic Electricity. McGraw-Hill Book Co., Inc., 1939, pp. 266-271.

6. Glauert, H.: The Elements of Aerofoil and Airscrew Theory. Cambridge Univ. Press, 1937, p. 204.

7. von Kármán, Th., and Burgers, J. M.: General Aerodynamic Theory - Perfect Fluids. Mathematical Foundation of the Theory of Wings with Finite Span. Vol. II of Aerodynamic Theory, div. E, ch. III, sec. 3, W. F. Durand, ed., Julius Springer (Berlin), 1935, pp. 103-104.

8. Ribner, Herbert S.: Propellers in Yaw. NACA ARR No. 3L09, 1943.

9. Munk, Max M.: Fundamentals of Fluid Dynamics for Aircraft Designers. The Ronald Press Co., 1929. pp. 15-23.

TABLE I

COMPARISON OF COMPUTED VALUES OF w' AND MEASURED VOLTAGE E

[$\alpha = 90°$; $\gamma = 0$; $z = 0$]

x (radii)	w'	E	K = w'/E
2.0	0.04411	0.03225	1.367
2.5	.02583	.01894	1.363
3.0	.01690	.01230	1.371
3.5	.01184	.00855	1.384
4.0	.00872	.00640	1.363
4.5	.00664	.00490	1.354
Average value of K = 1.366			

NATIONAL ADVISORY
COMMITTEE FOR AERONAUTICS

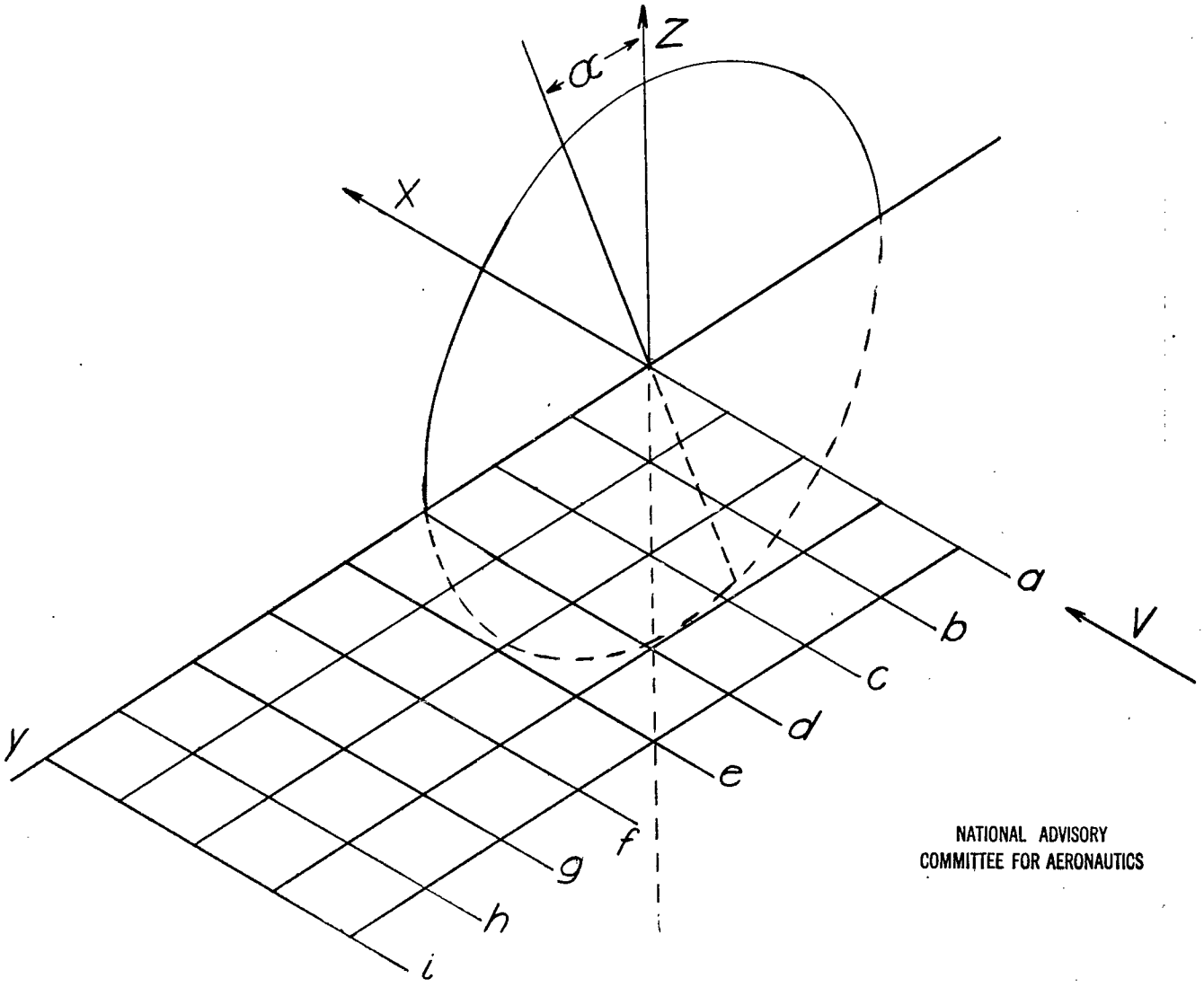

Figure 1.- Orientation of axes and location of measuring planes.

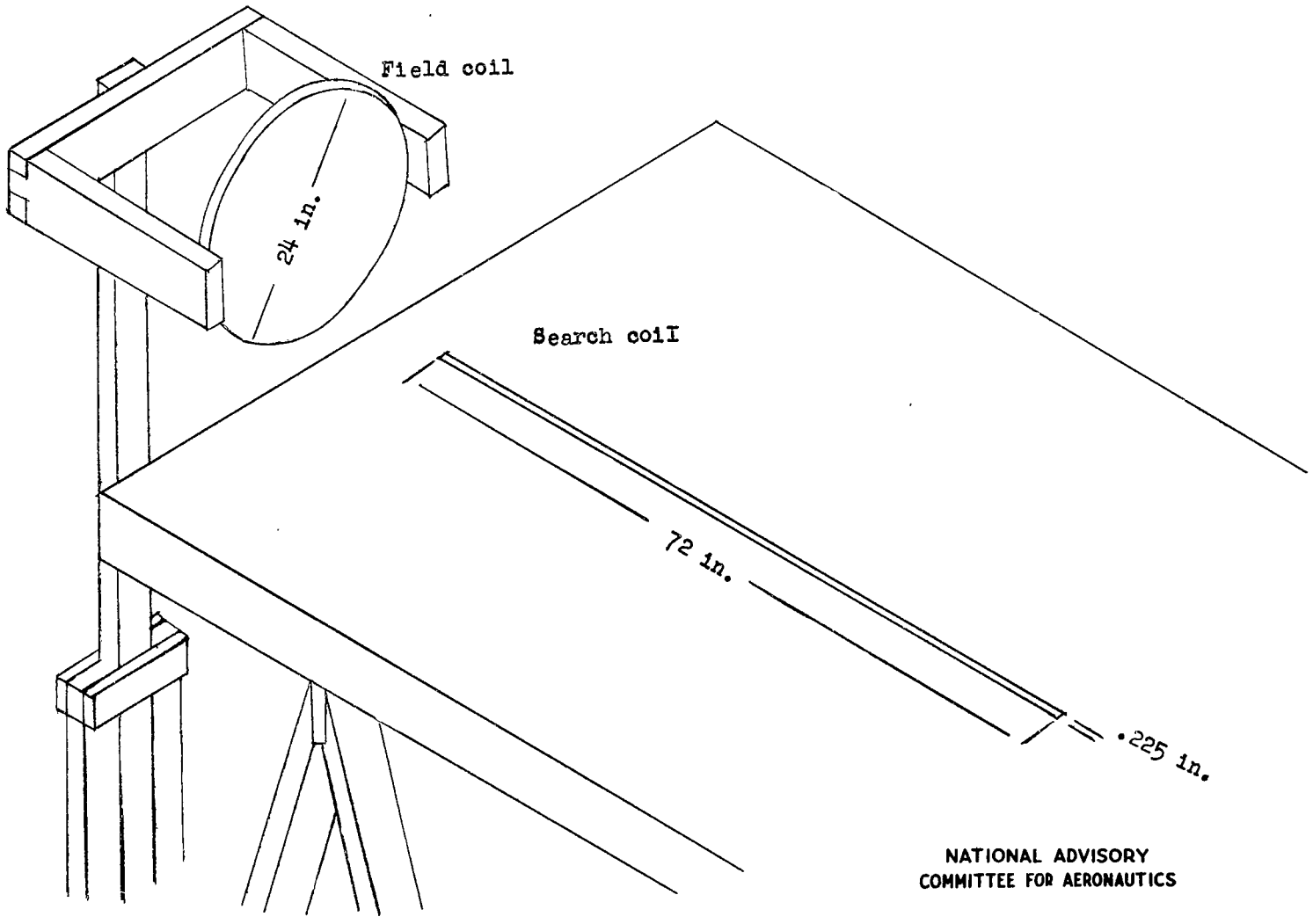

Figure 2.- Schematic diagram of setup.

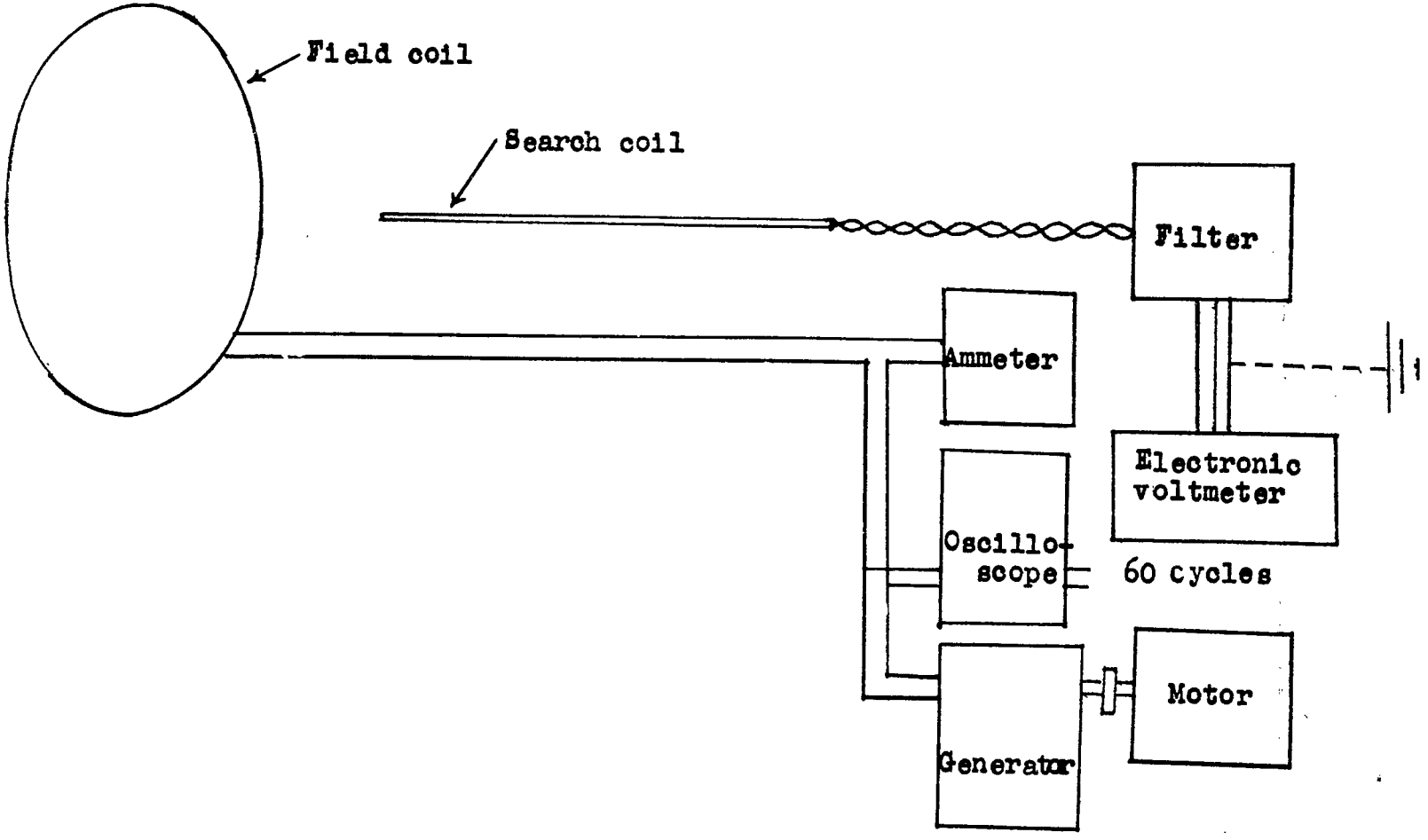

Figure 3.- Electric circuit.

NATIONAL ADVISORY
COMMITTEE FOR AERONAUTICS

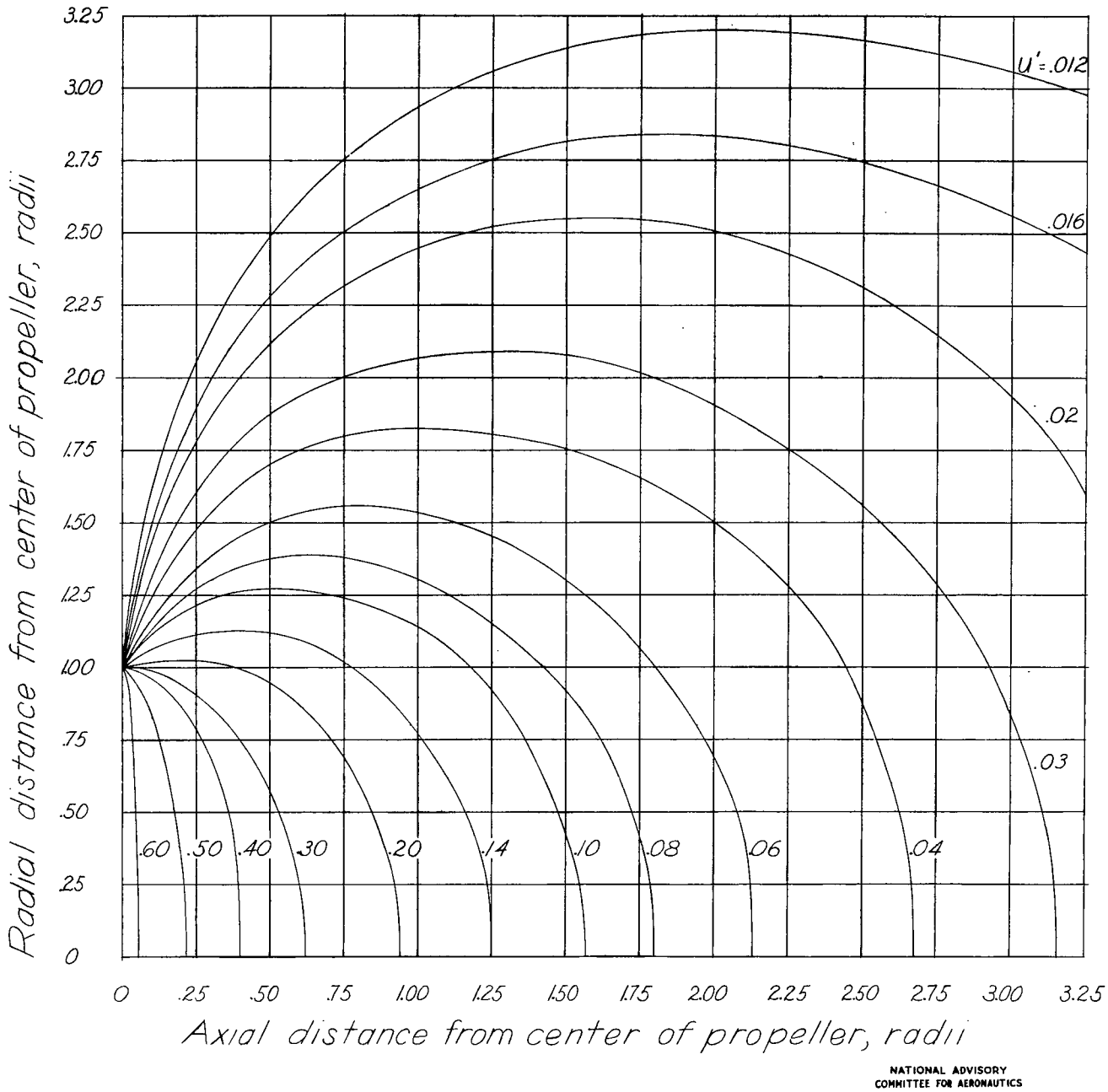

Figure 4.- Contours of horizontal velocity.

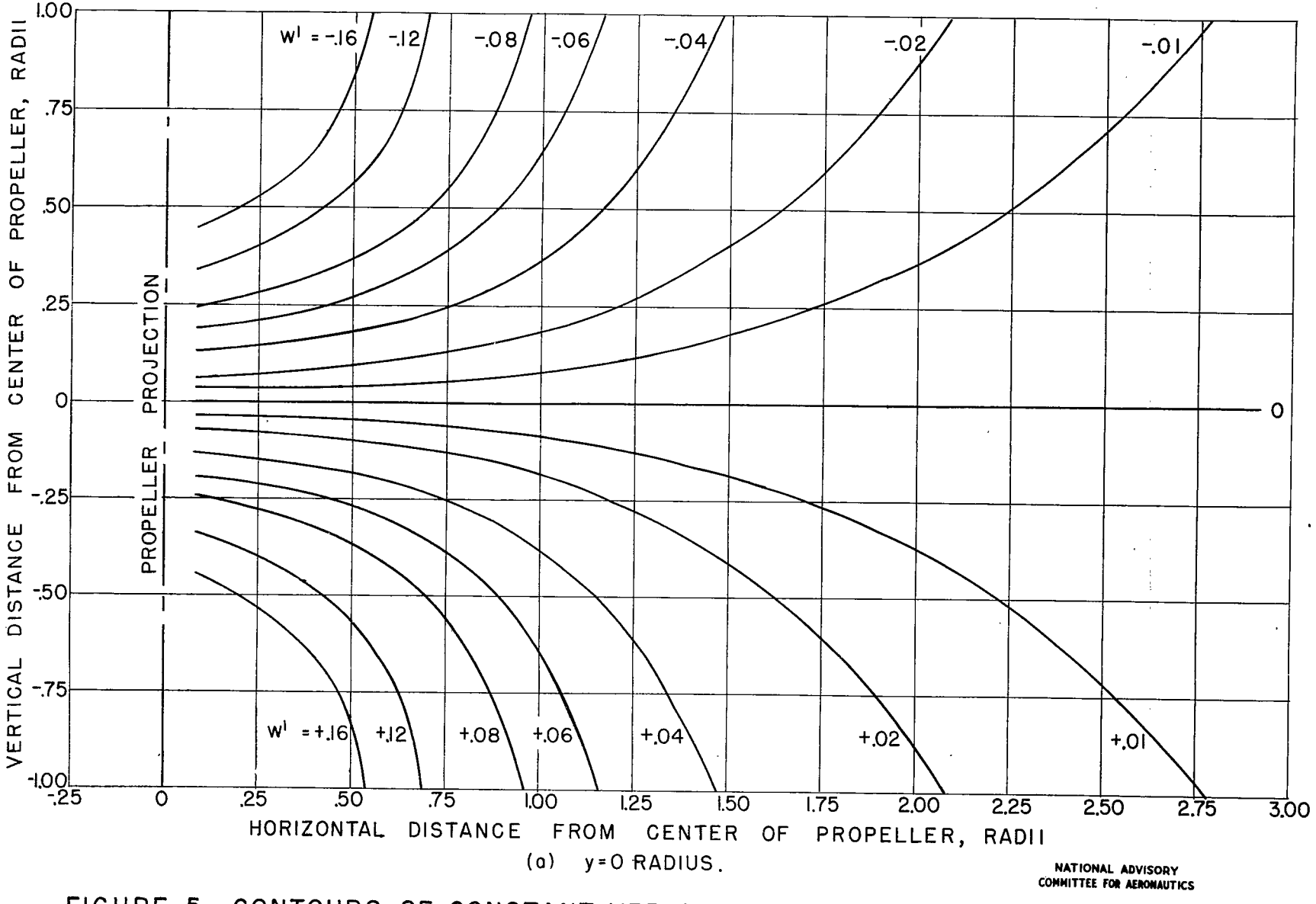

FIGURE 5.- CONTOURS OF CONSTANT VERTICAL VELOCITY FOR $\alpha = 0°$.

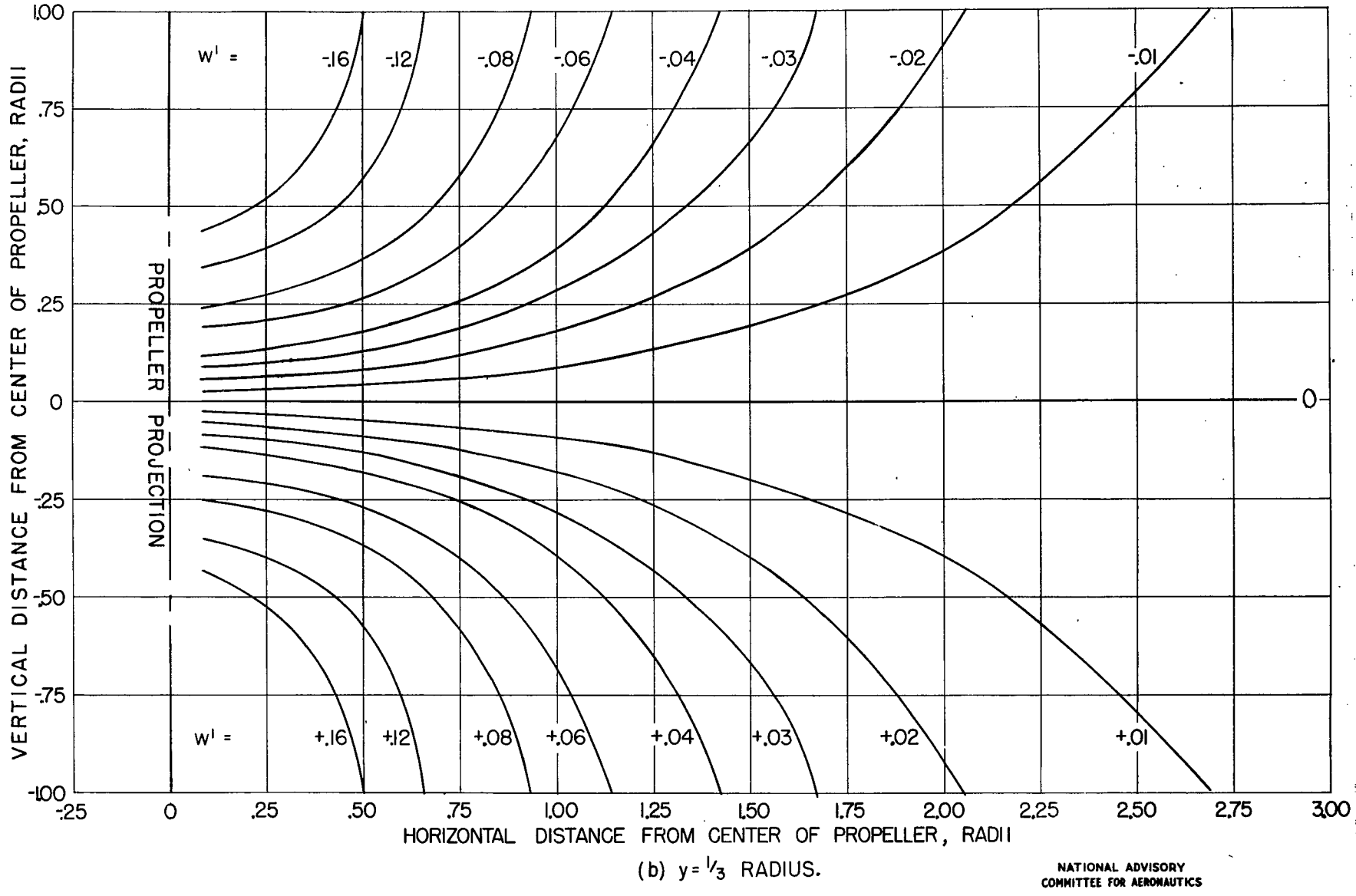

(b) $y = 1/3$ RADIUS.

NATIONAL ADVISORY COMMITTEE FOR AERONAUTICS

Fig. 5b

NACA ARR No. L6A05b

FIGURE 5.- CONTINUED.

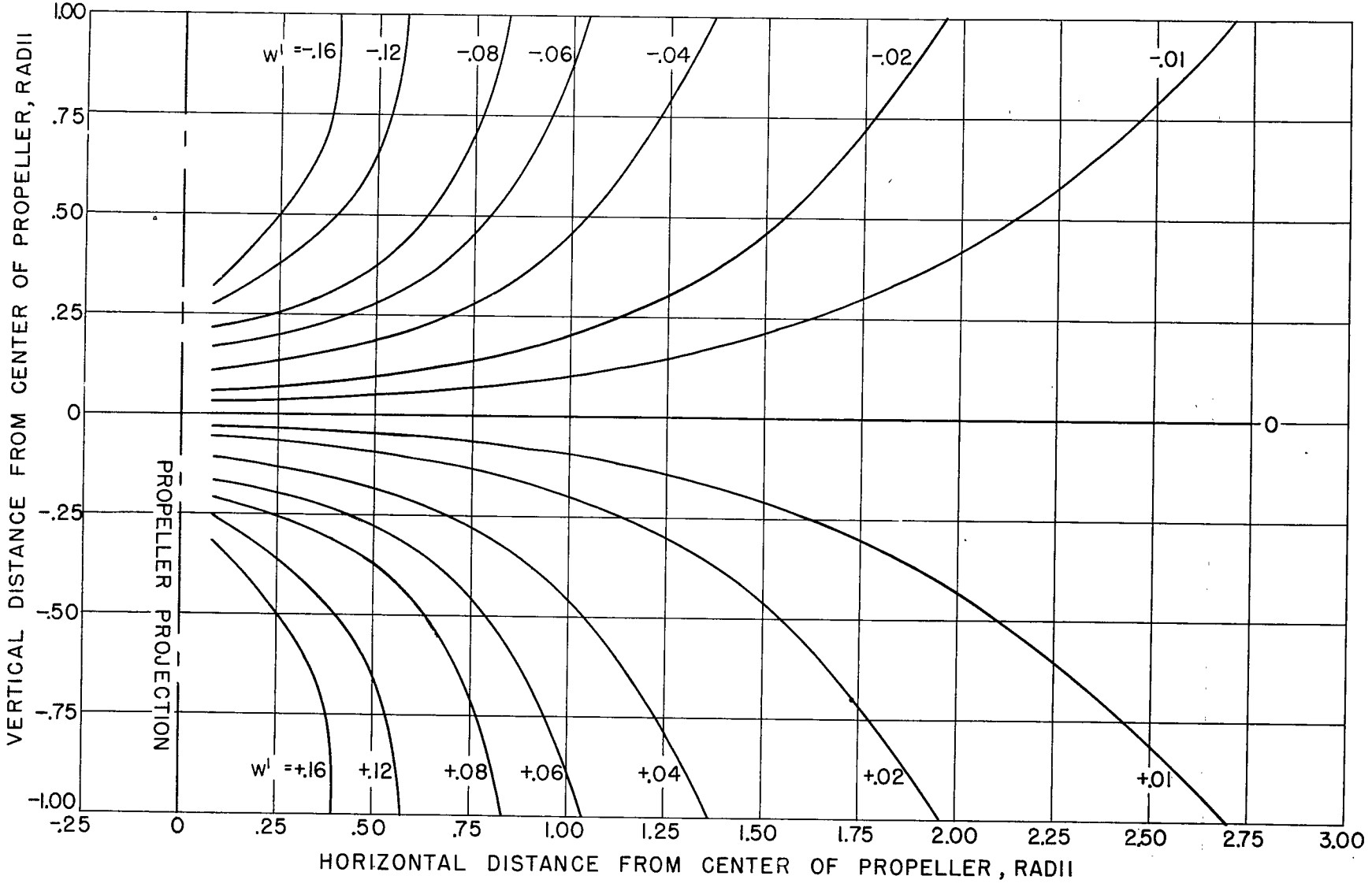

(c) $y = \frac{2}{3}$ RADIUS.

FIGURE 5.- CONTINUED.

NATIONAL ADVISORY
COMMITTEE FOR AERONAUTICS

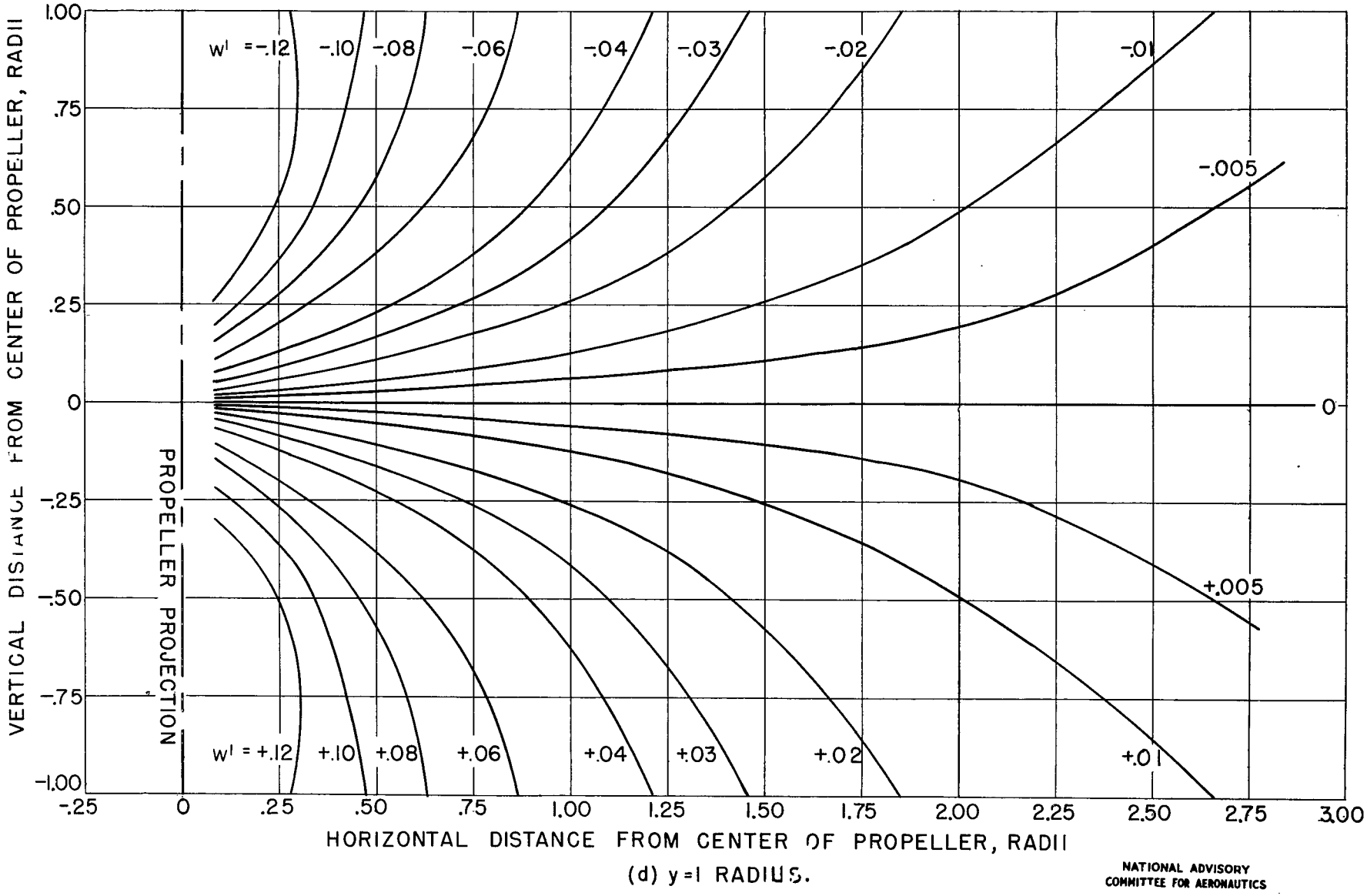

(d) y=1 RADIUS.

NATIONAL ADVISORY COMMITTEE FOR AERONAUTICS

FIGURE 5.- CONTINUED.

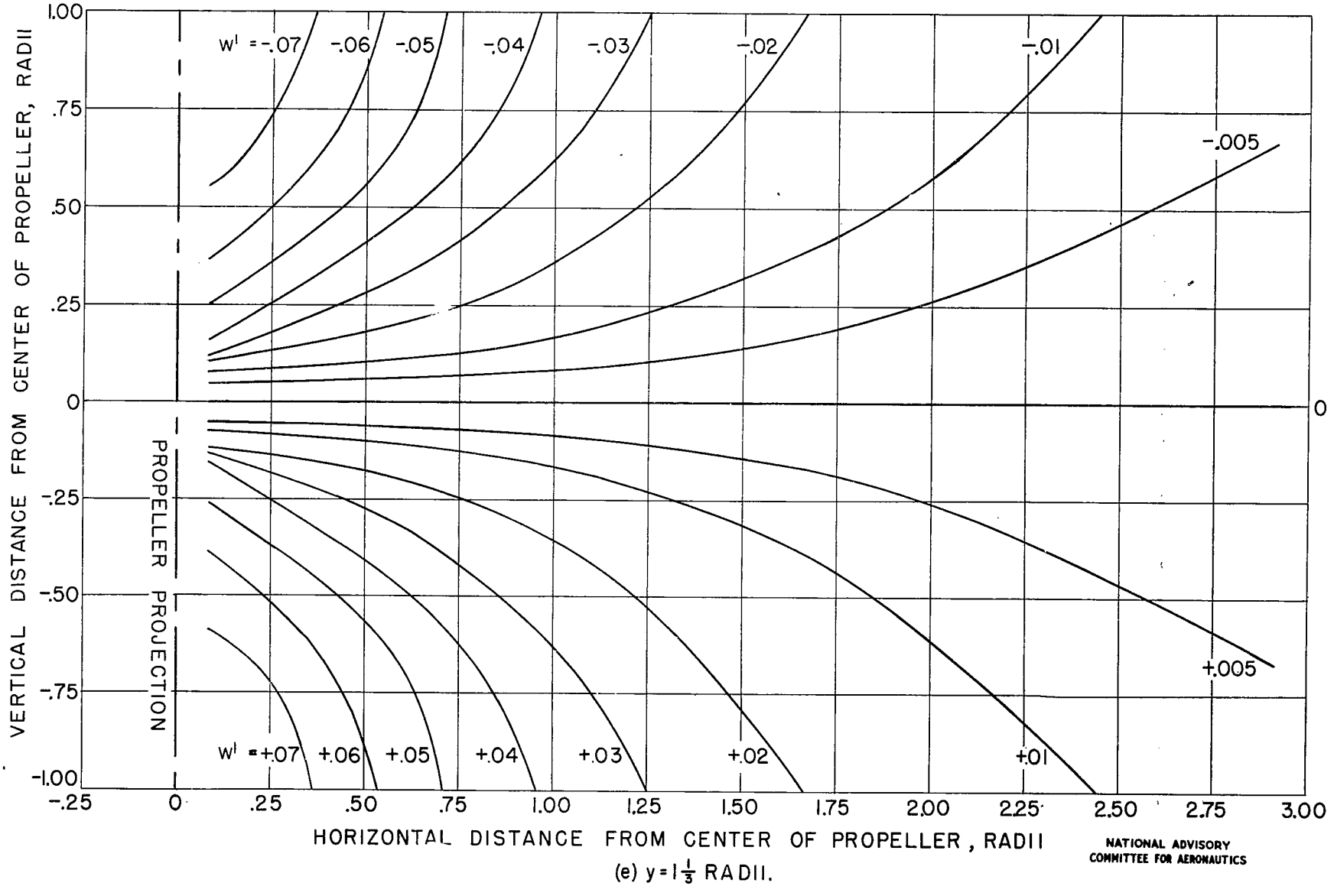

(e) $y = 1\frac{1}{3}$ RADII.

FIGURE 5.– CONTINUED.

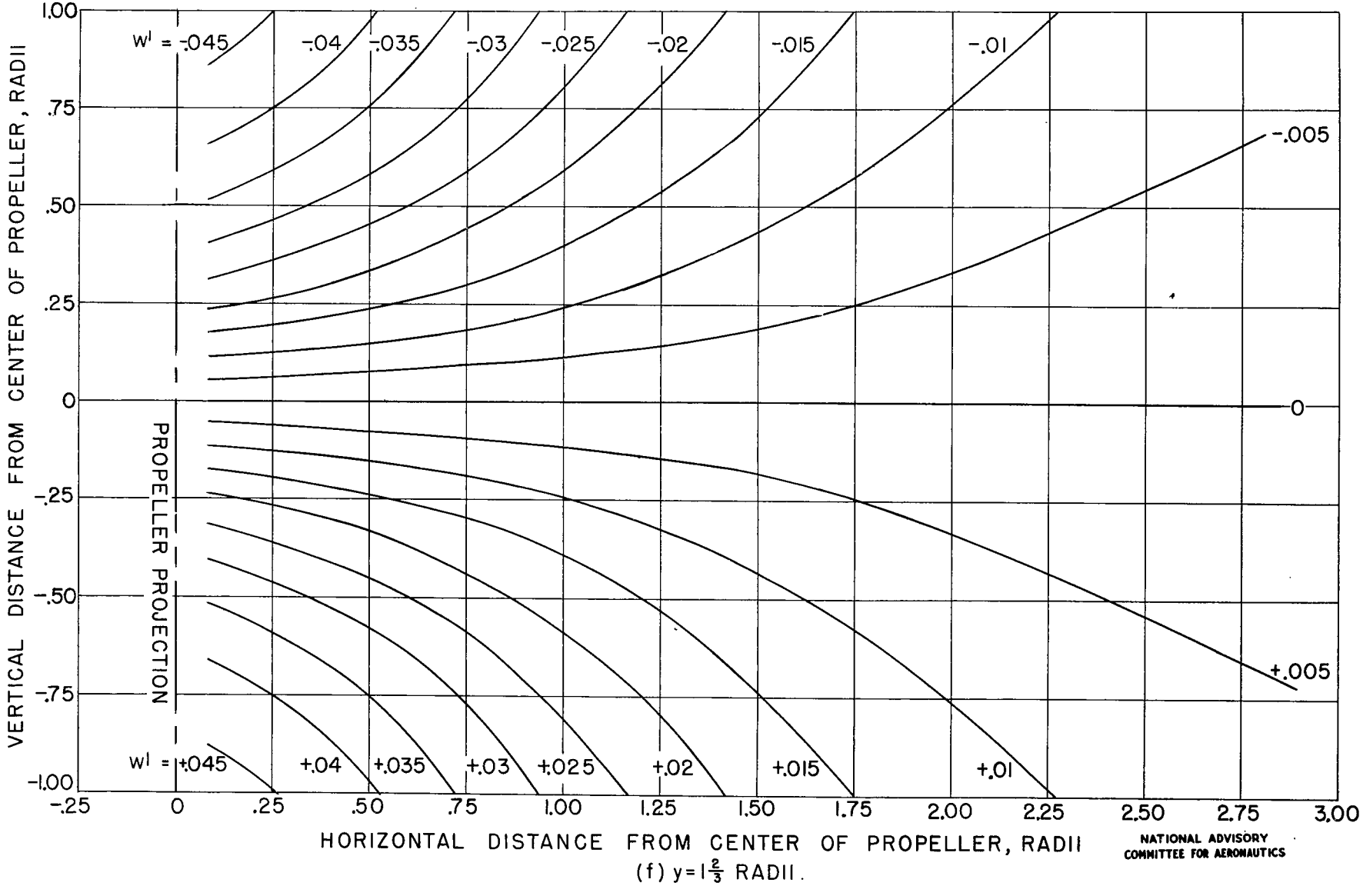

(f) $y = 1\frac{2}{3}$ RADII.

FIGURE 5.- CONTINUED.

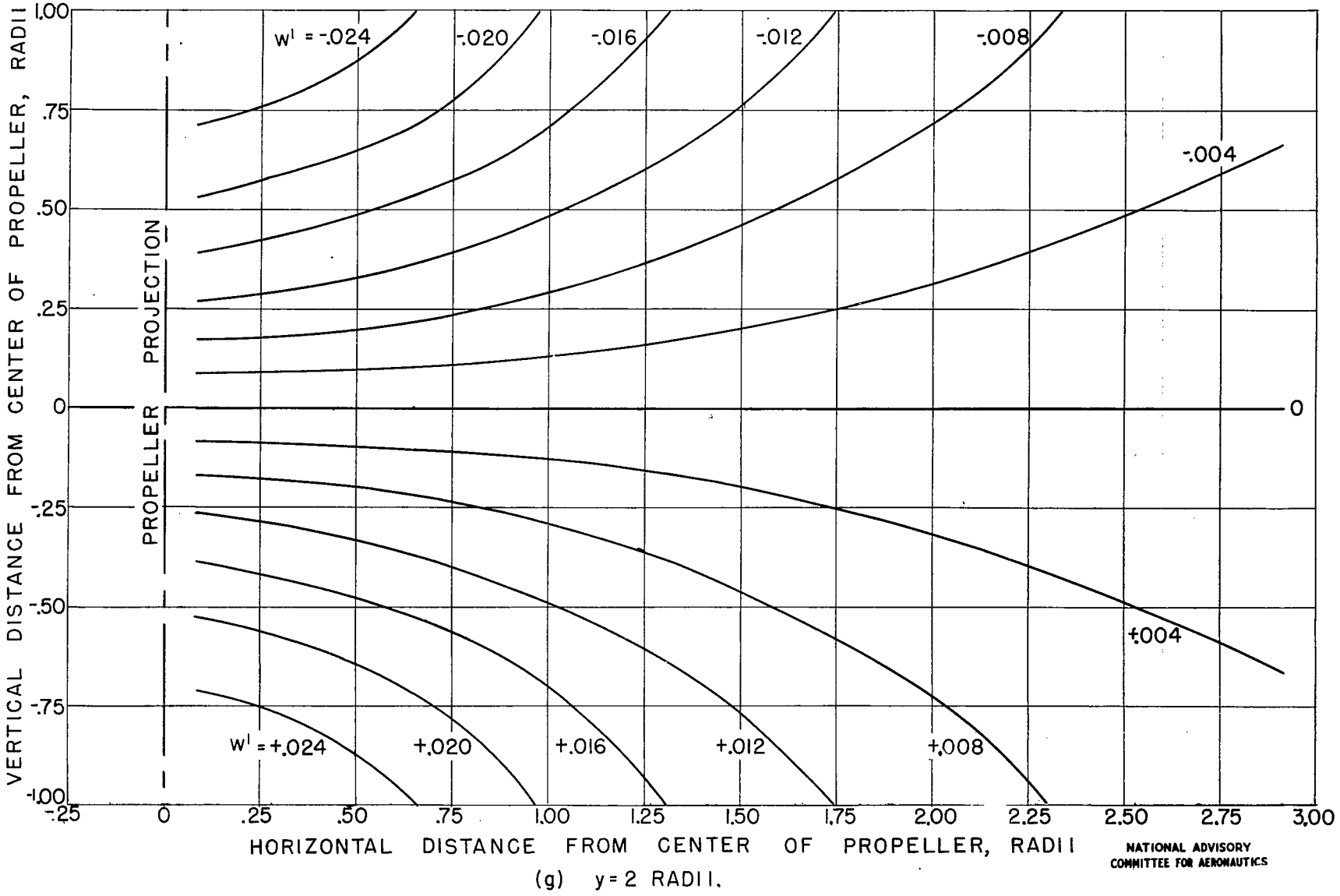

(g) y = 2 RADII.

FIGURE 5.- CONTINUED.

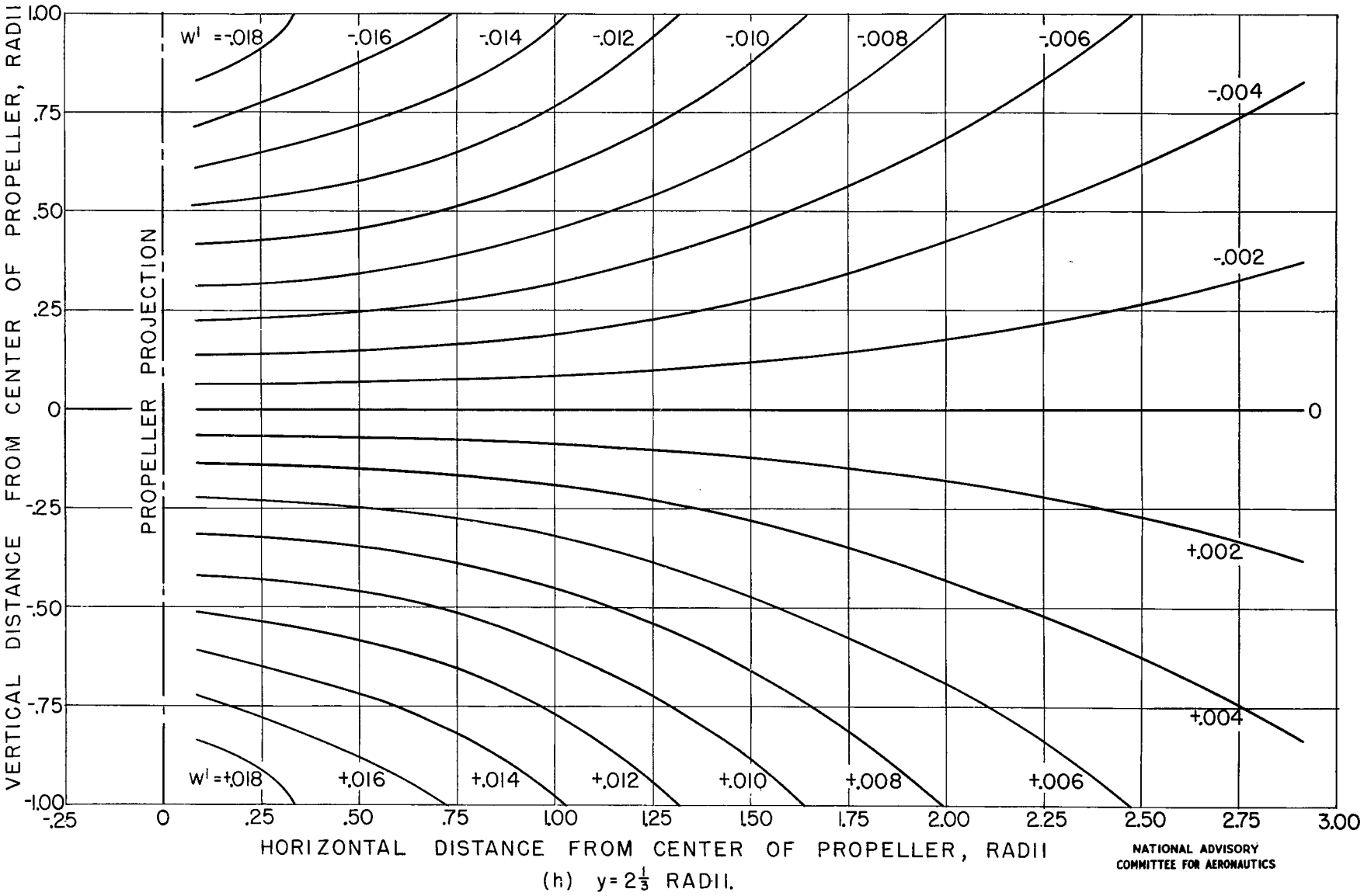

(h) $y = 2\frac{1}{3}$ RADII.

FIGURE 5,- CONTINUED.

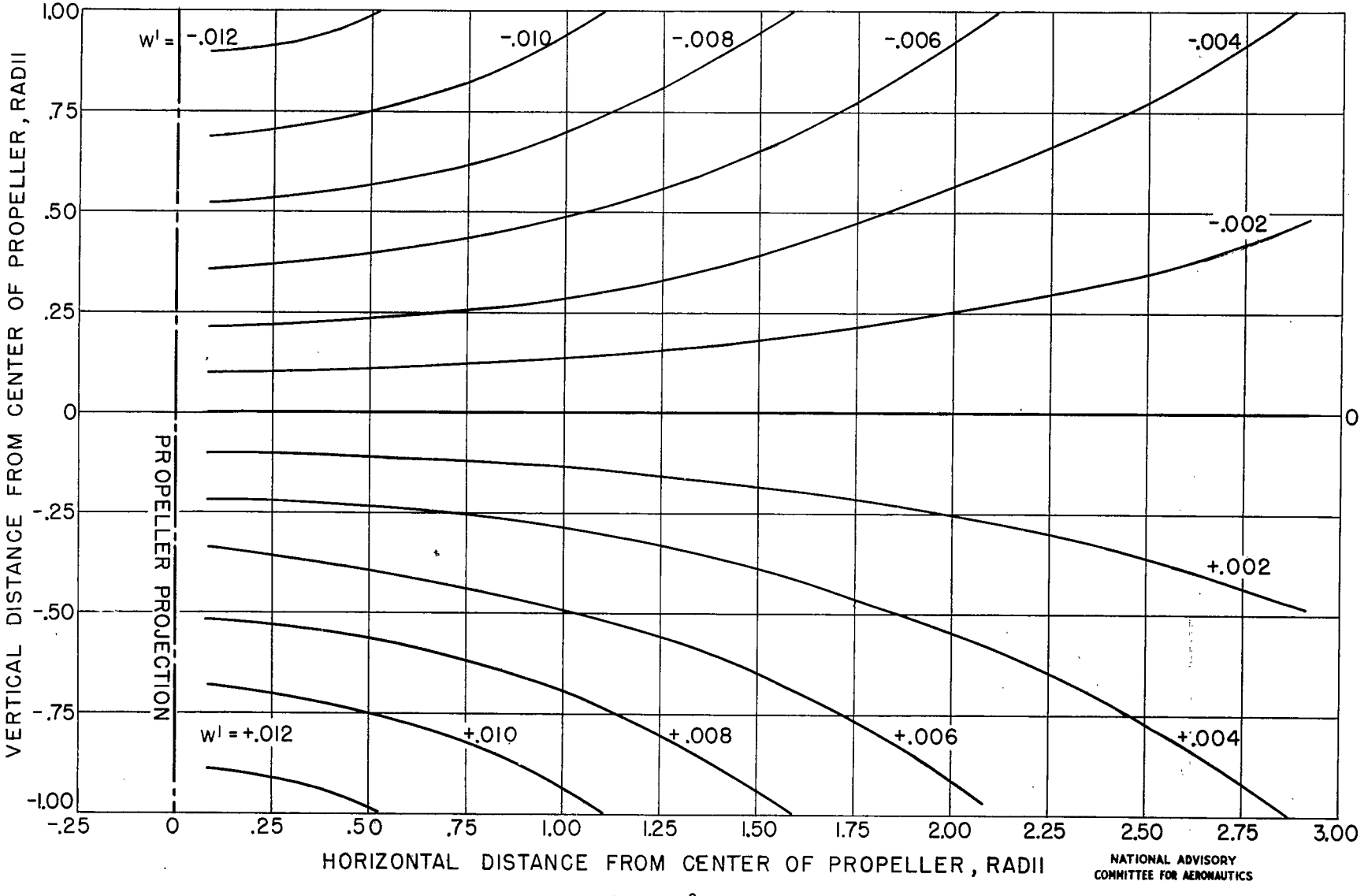

(i) $y = 2\frac{2}{3}$ RADII.

FIGURE 5.- CONCLUDED.

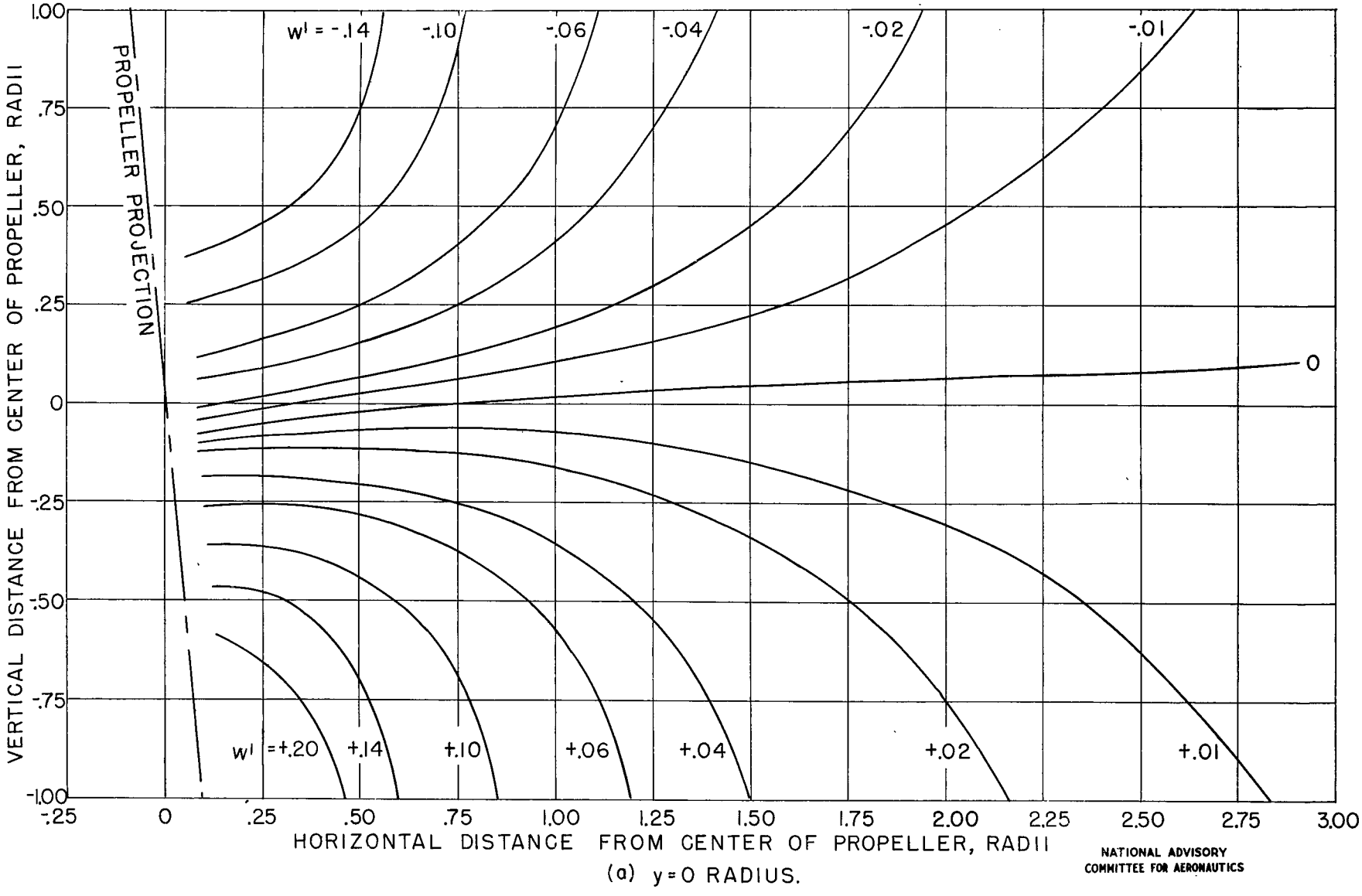

(a) y = 0 RADIUS.

FIGURE 6.- CONTOURS OF CONSTANT VERTICAL VELOCITY FOR $\alpha = 5°$.

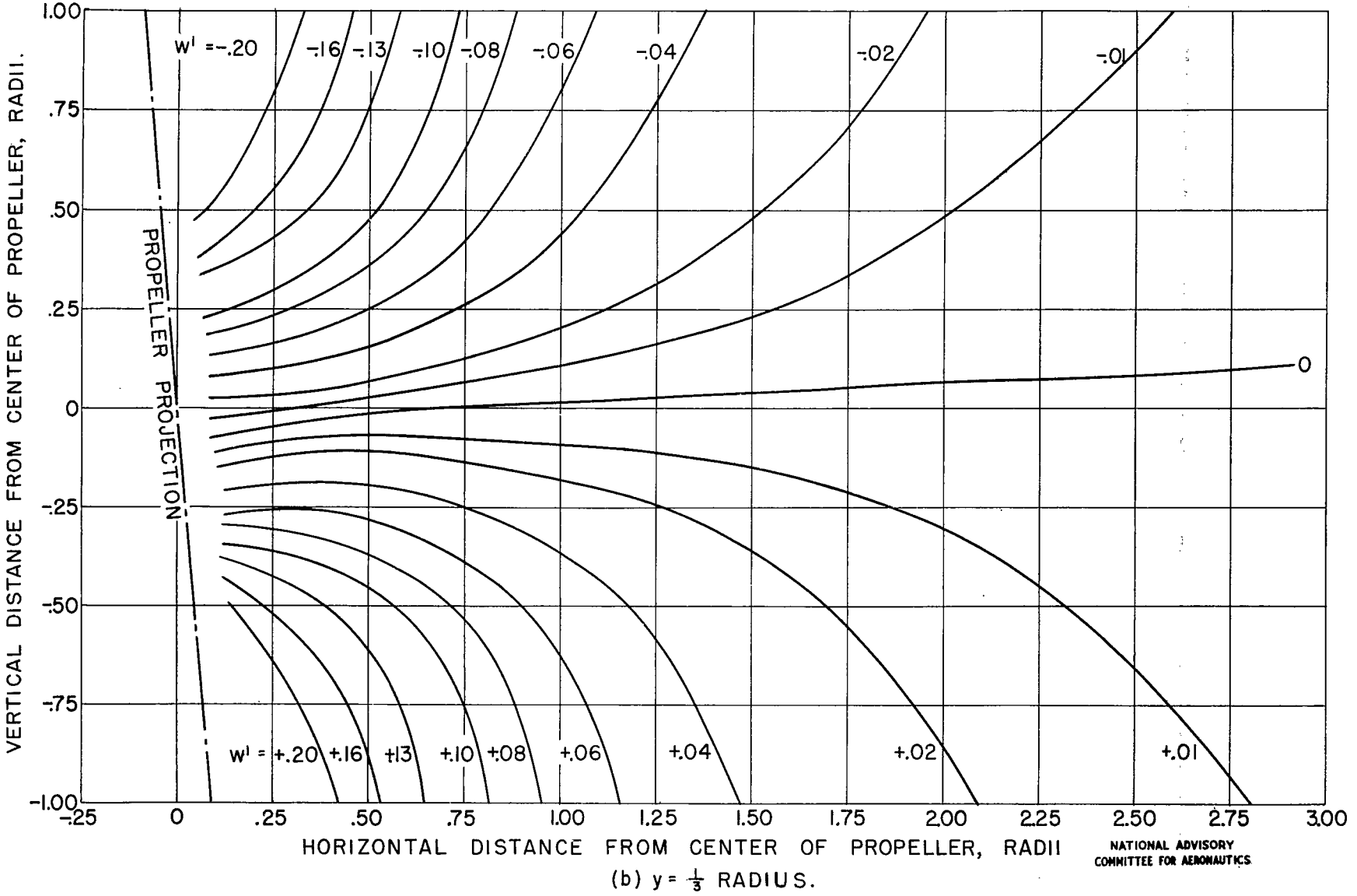

(b) $y = \frac{1}{3}$ RADIUS.

FIGURE 6.- CONTINUED.

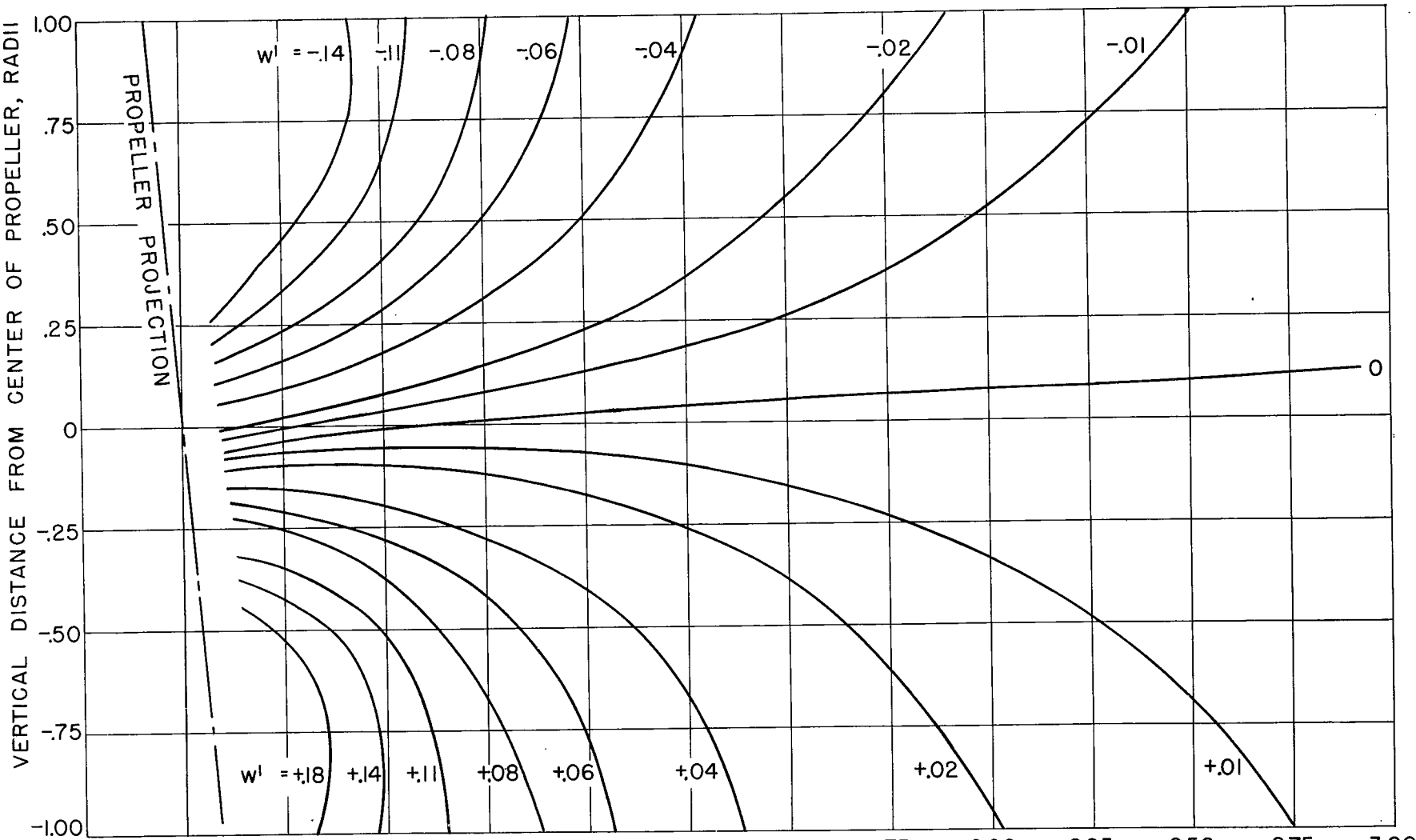

(c) $y=\frac{2}{3}$ RADIUS.

FIGURE 6.- CONTINUED.

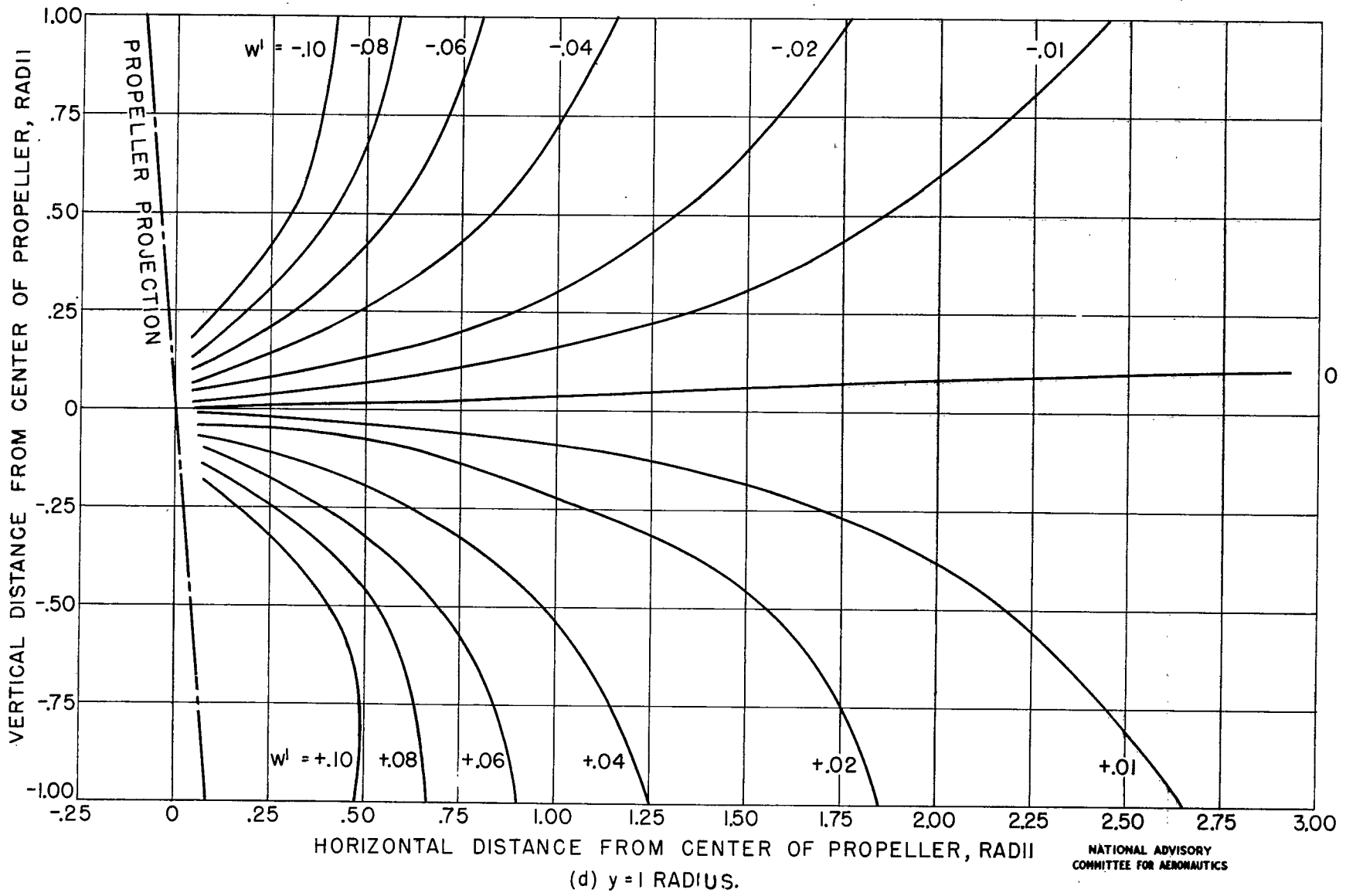

(d) y = 1 RADIUS.

FIGURE 6.- CONTINUED.

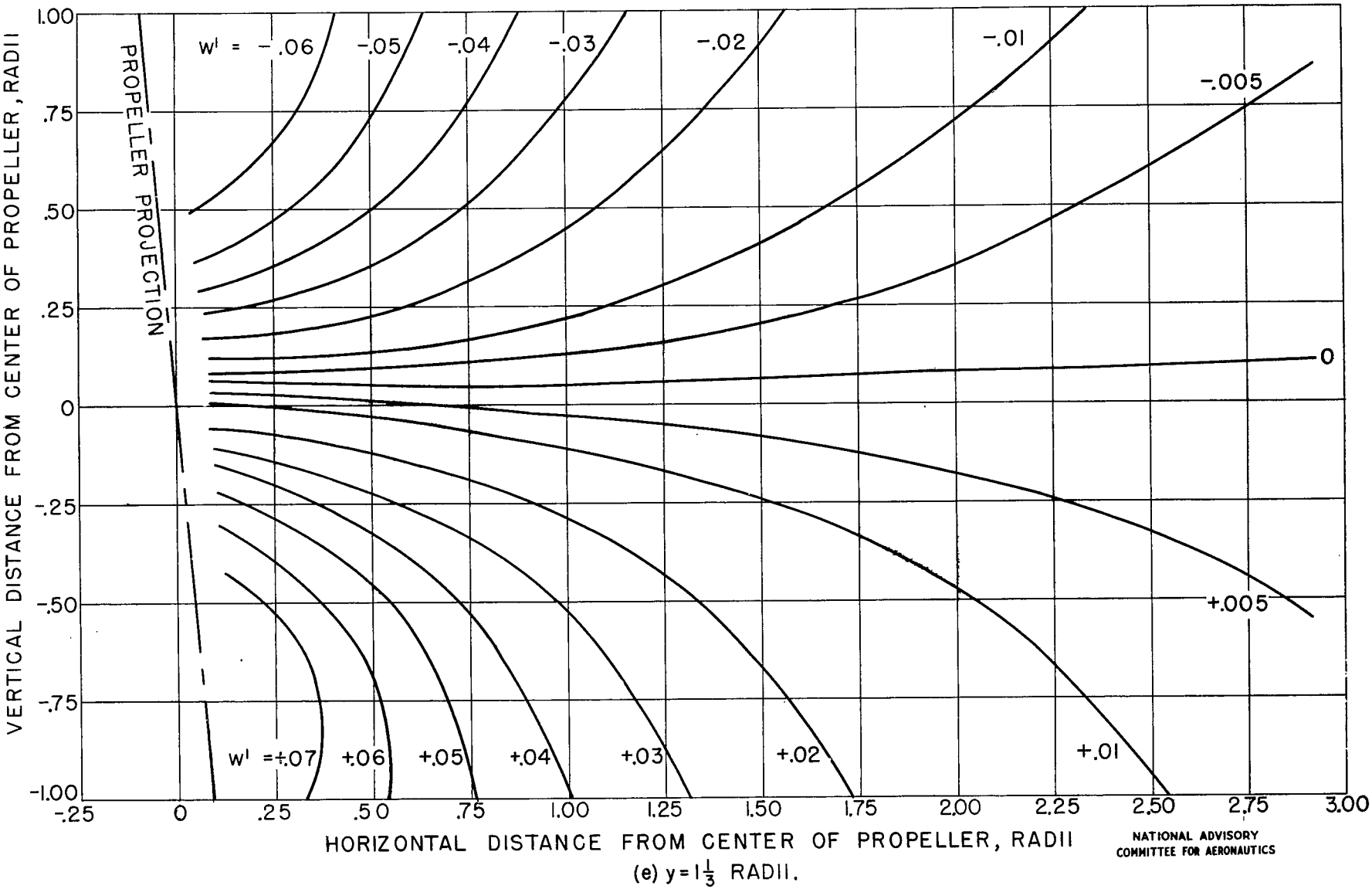

(e) $y = 1\frac{1}{3}$ RADII.

FIGURE 6.- CONTINUED.

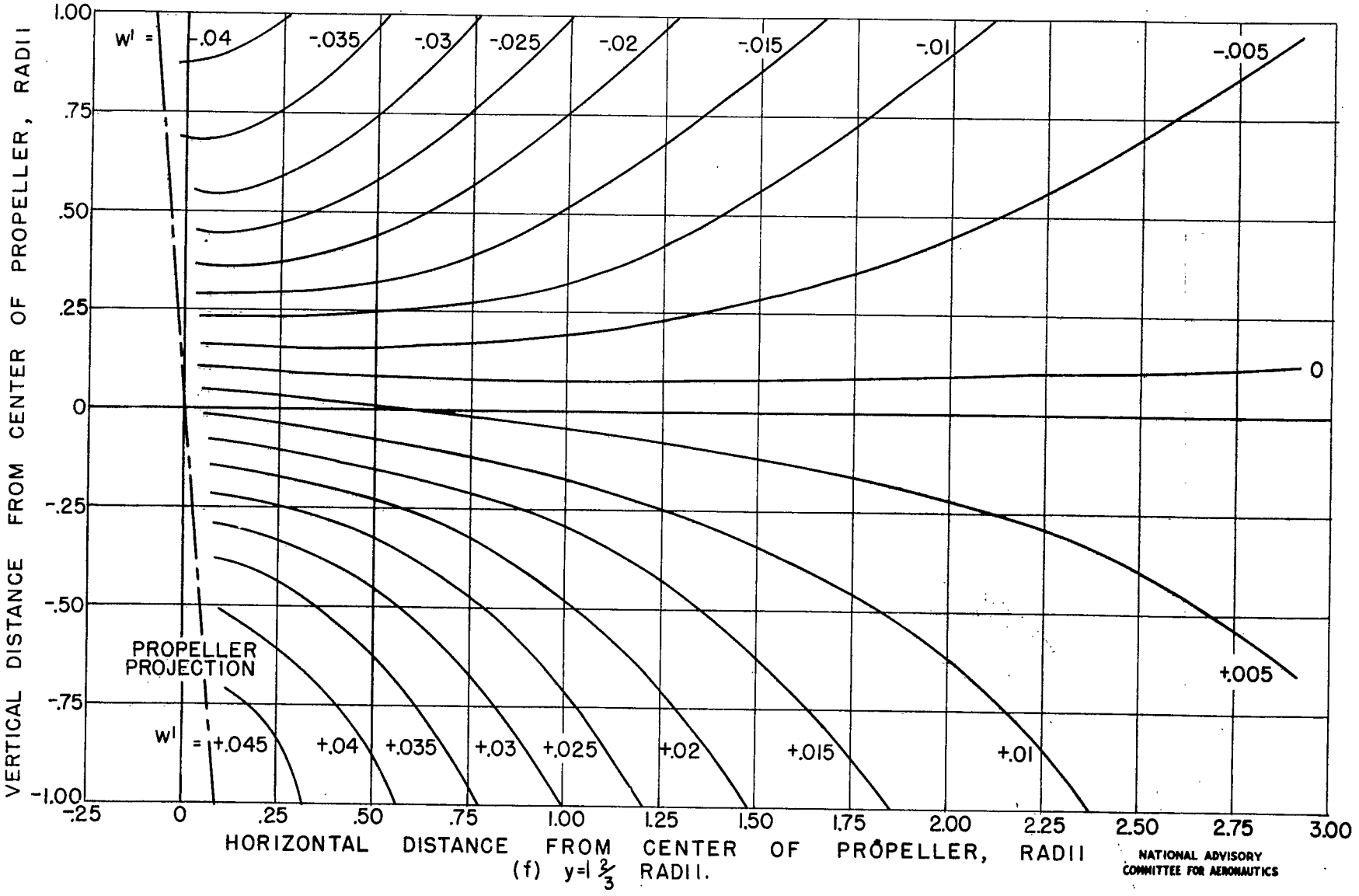

FIGURE 6.- CONTINUED.

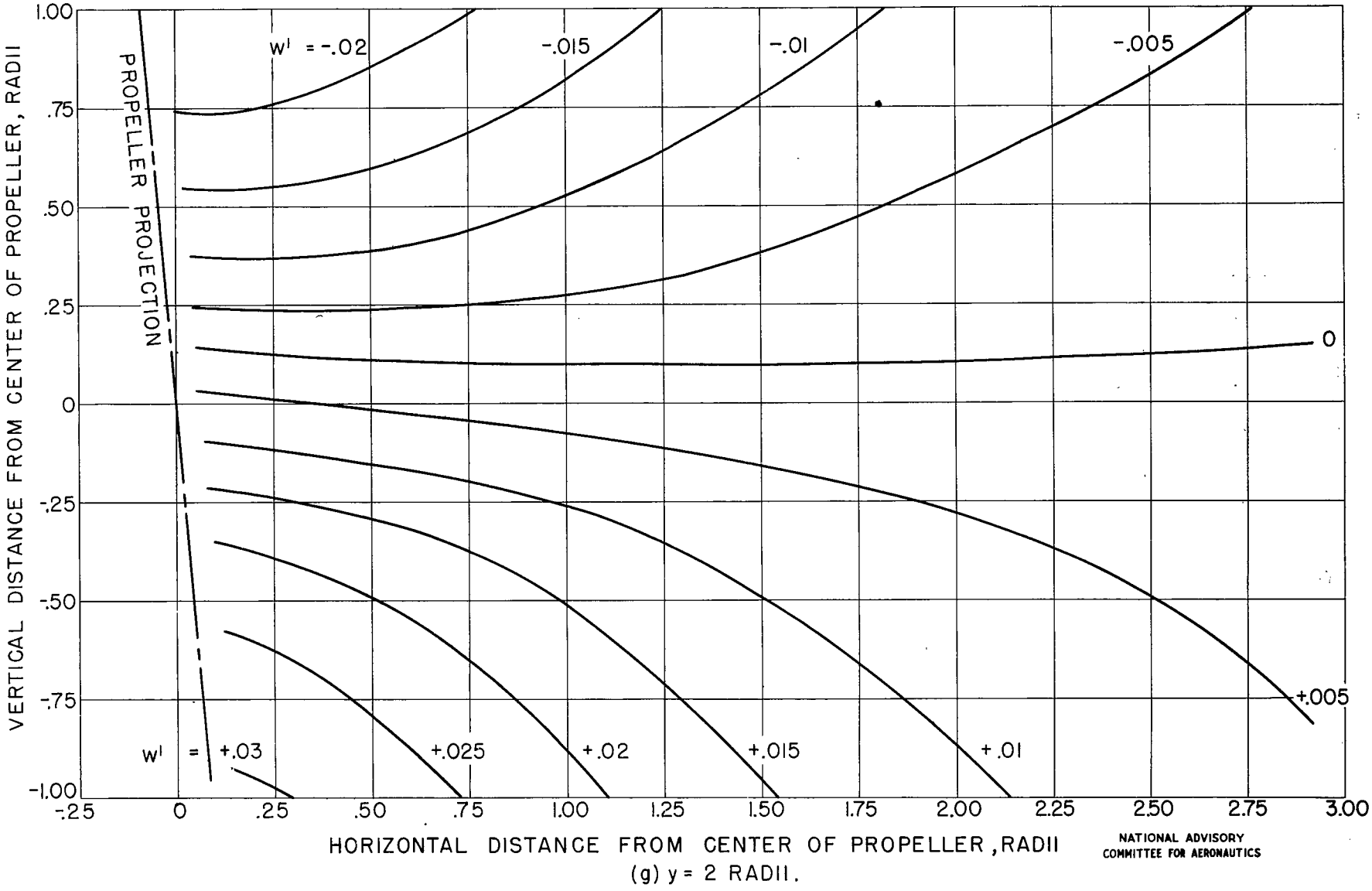

(g) y = 2 RADII.

FIGURE 6.- CONTINUED.

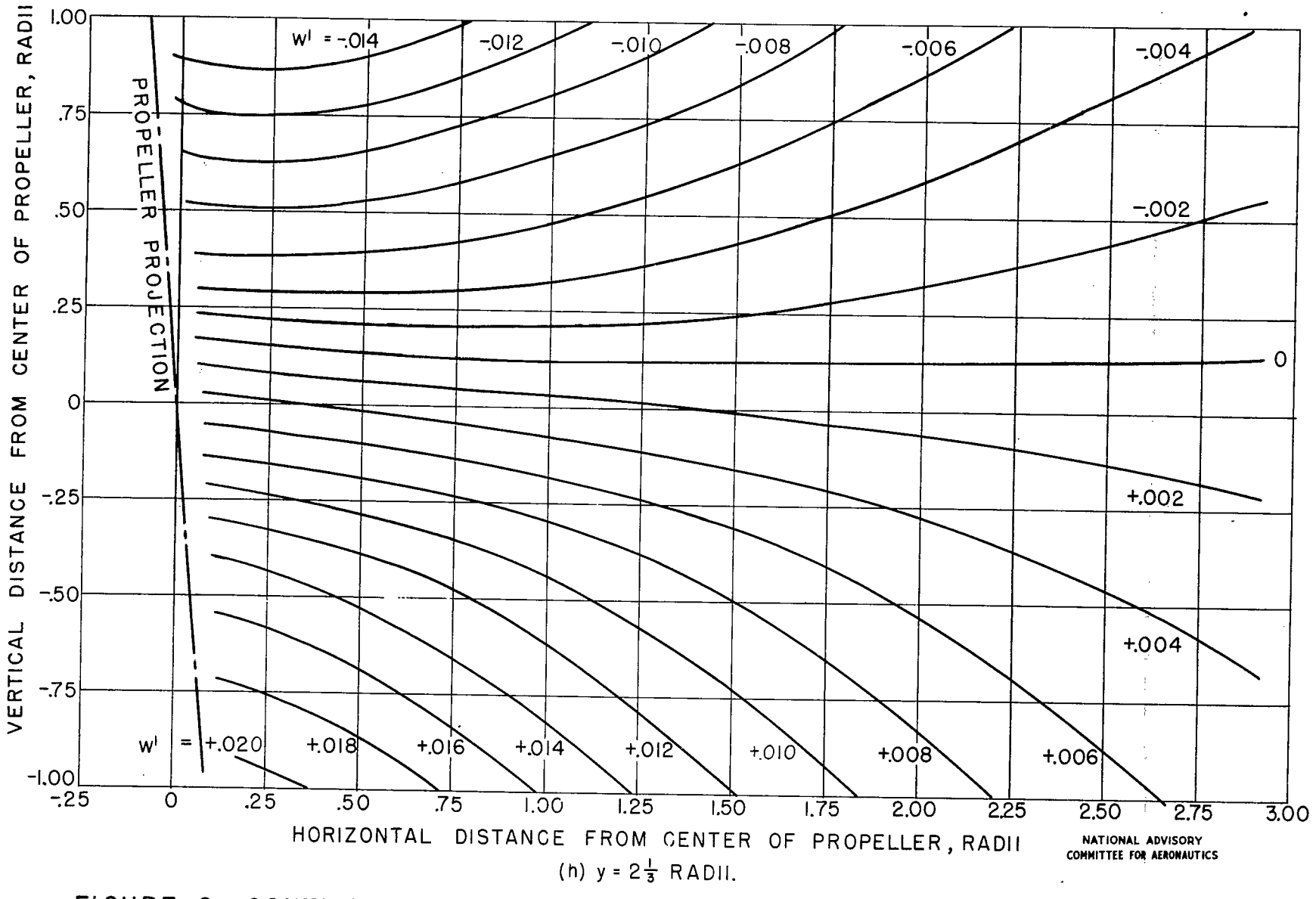

(h) $y = 2\frac{1}{3}$ RADII.

FIGURE 6.- CONTINUED.

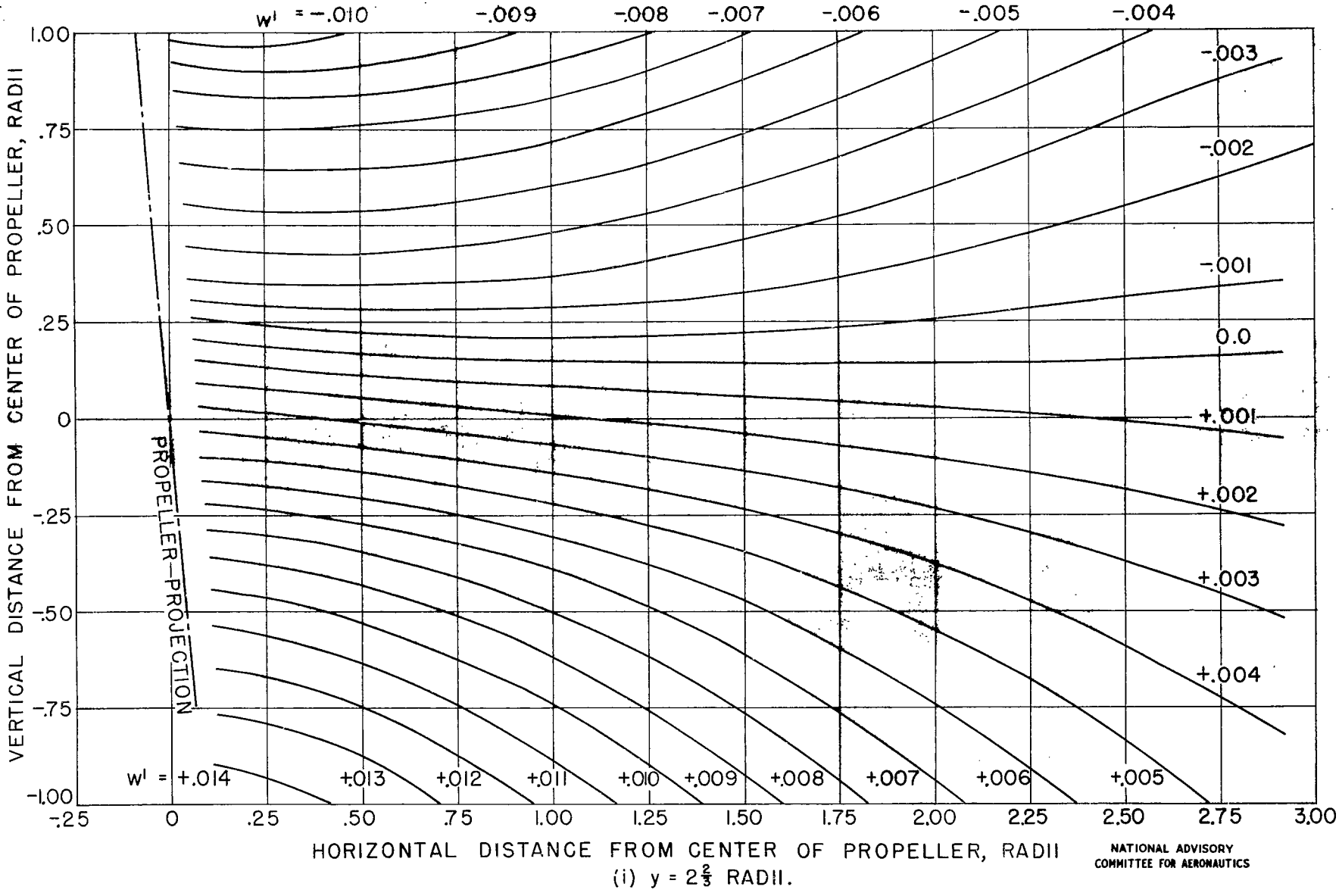

(i) $y = 2\frac{2}{3}$ RADII.

FIGURE 6.- CONCLUDED.

Fig. 6i

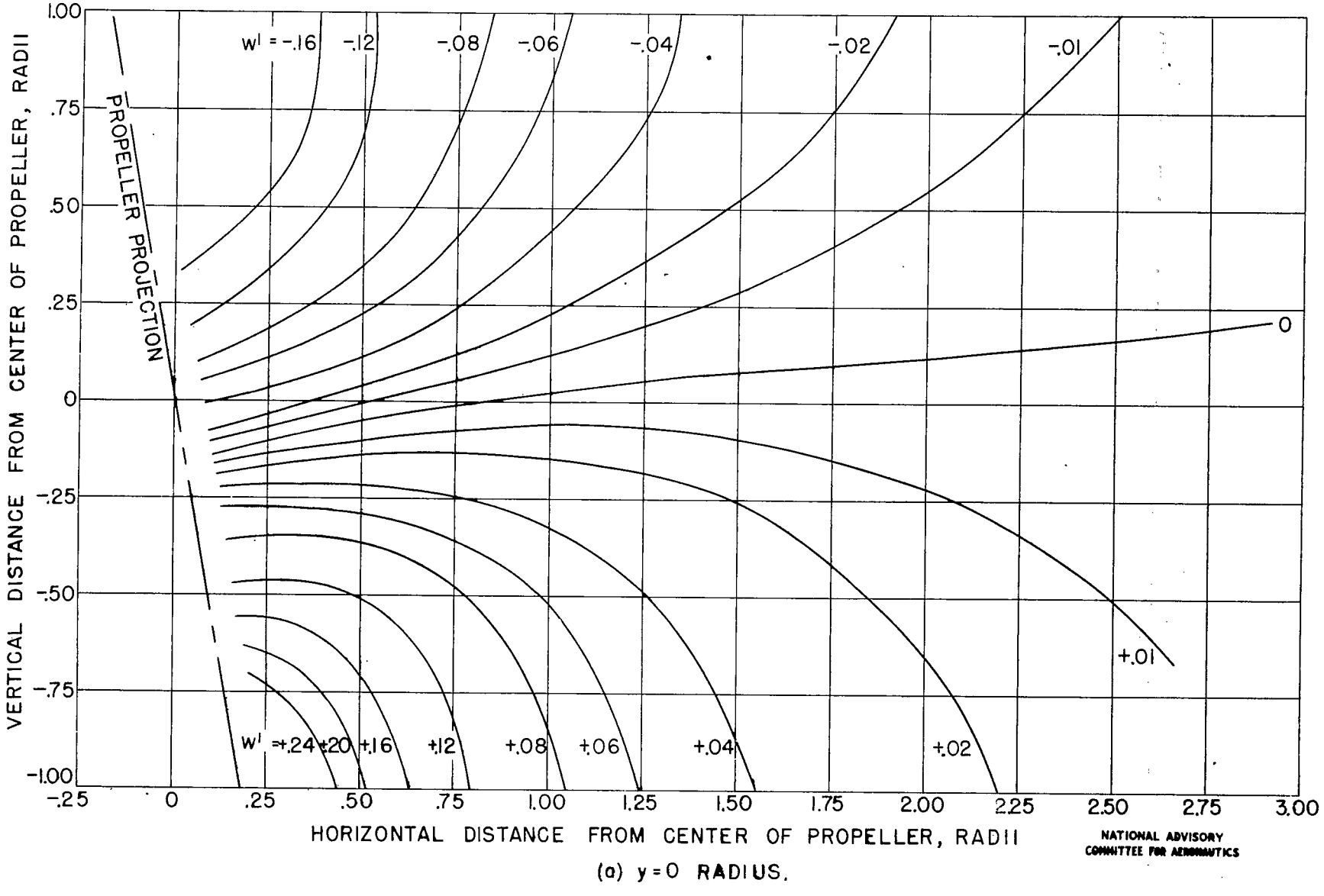

(a) y = 0 RADIUS.

FIGURE 7.- CONTOURS OF CONSTANT VERTICAL VELOCITY FOR $\alpha = 10°$

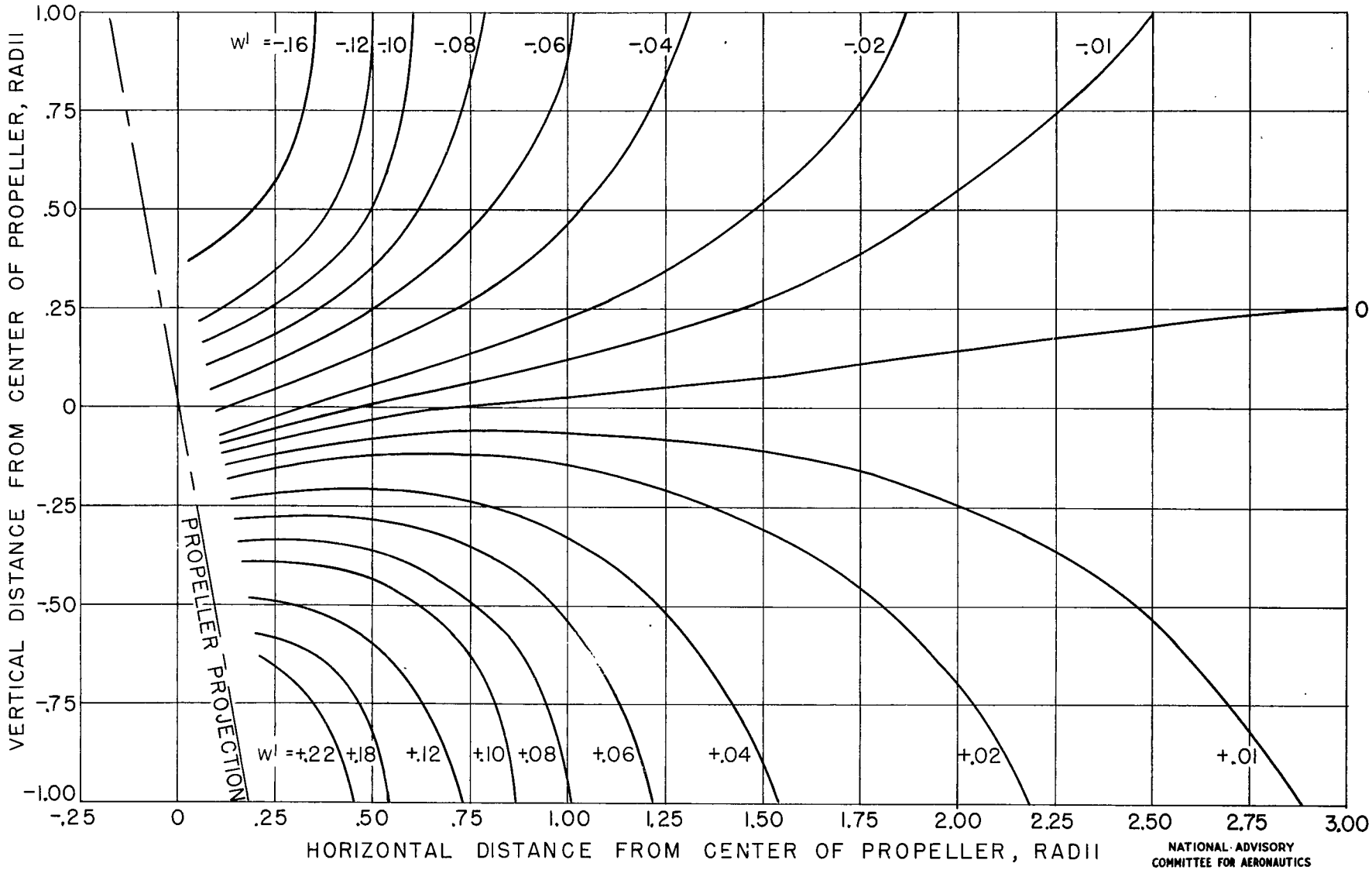

(b) $y = \frac{1}{3}$ RADIUS.

FIGURE 7.- CONTINUED.

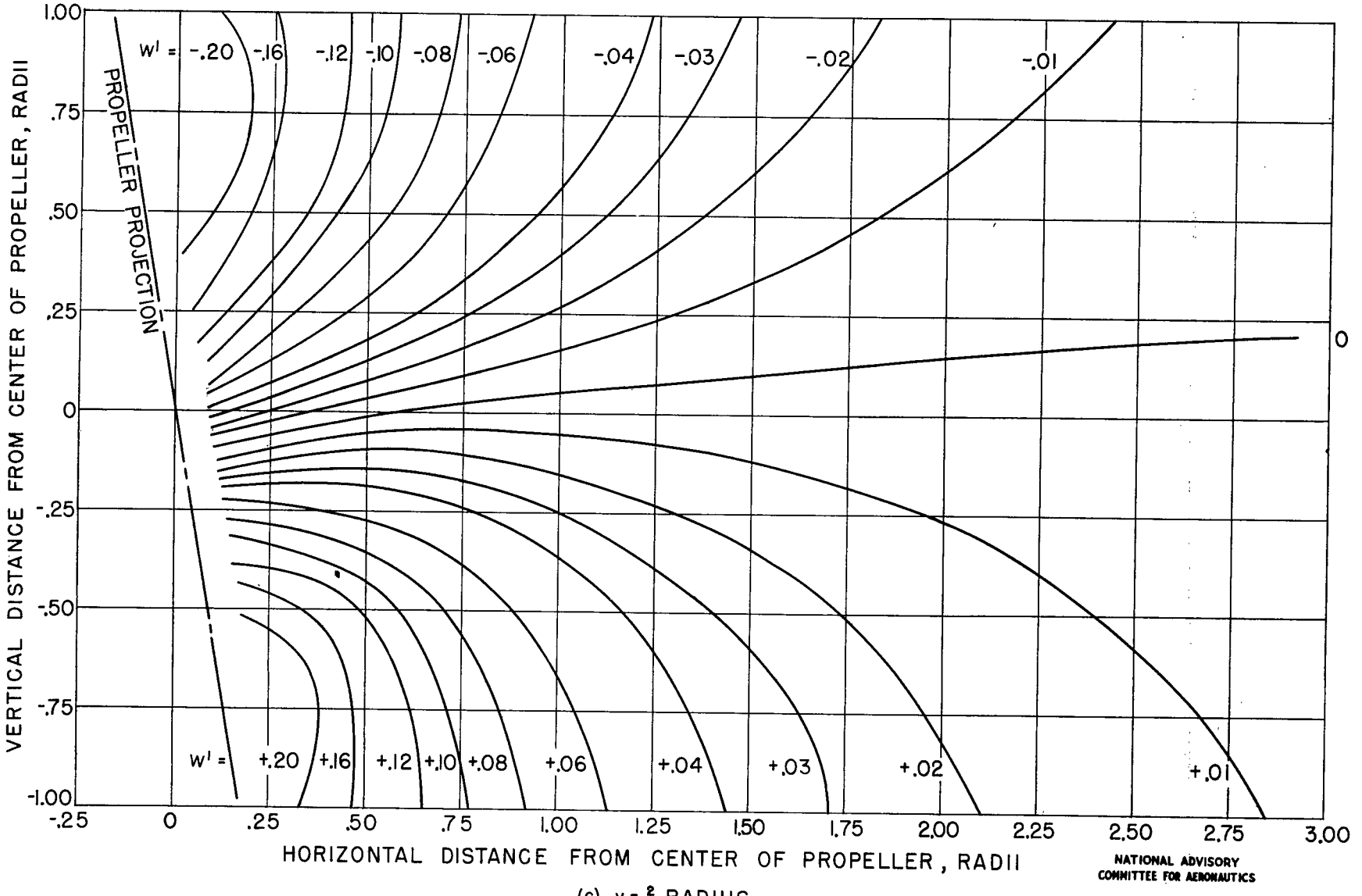

(c) $y = \frac{2}{3}$ RADIUS.

FIGURE 7.- CONTINUED.

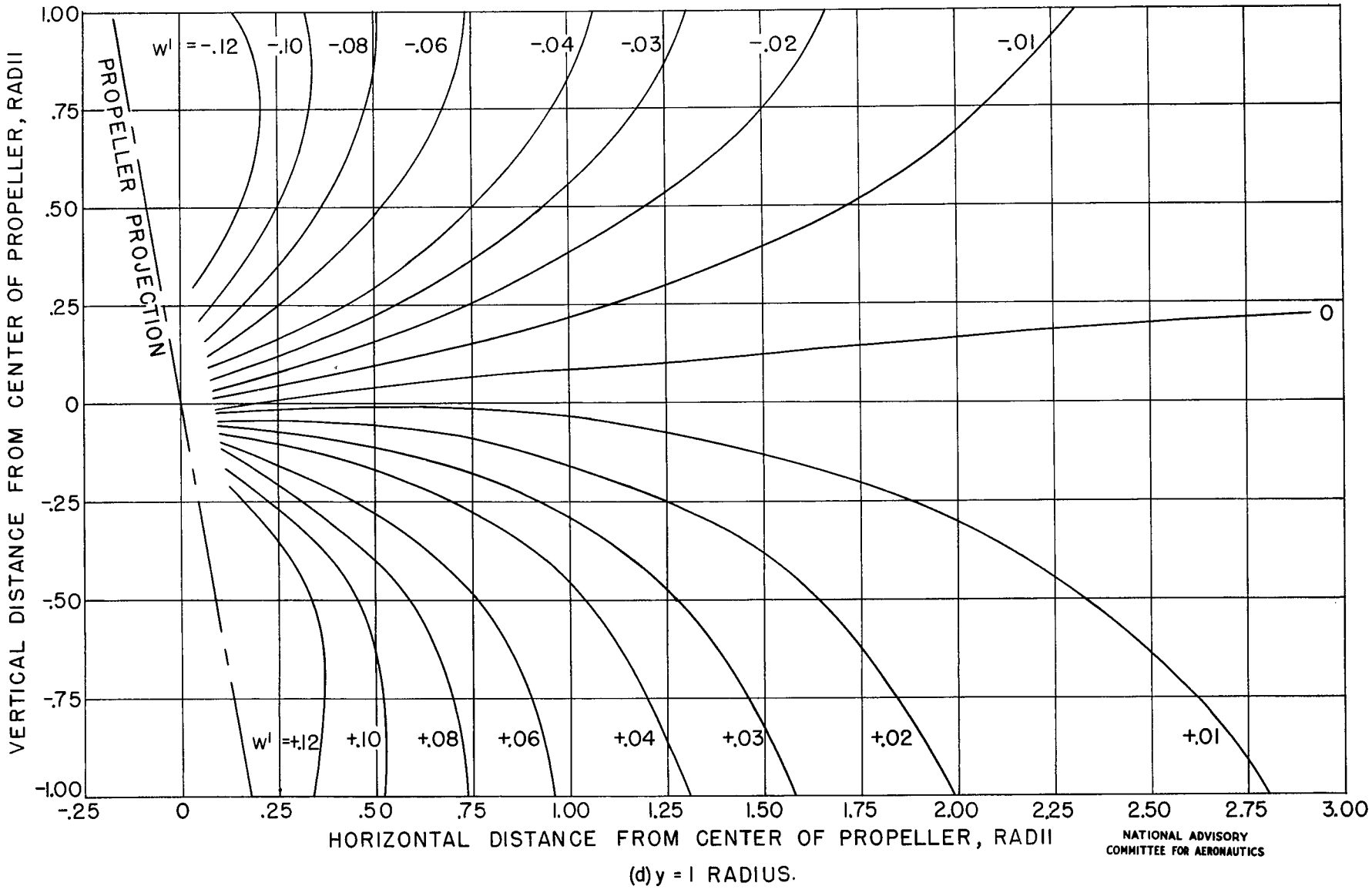

(d) y = 1 RADIUS.

FIGURE 7.- CONTINUED.

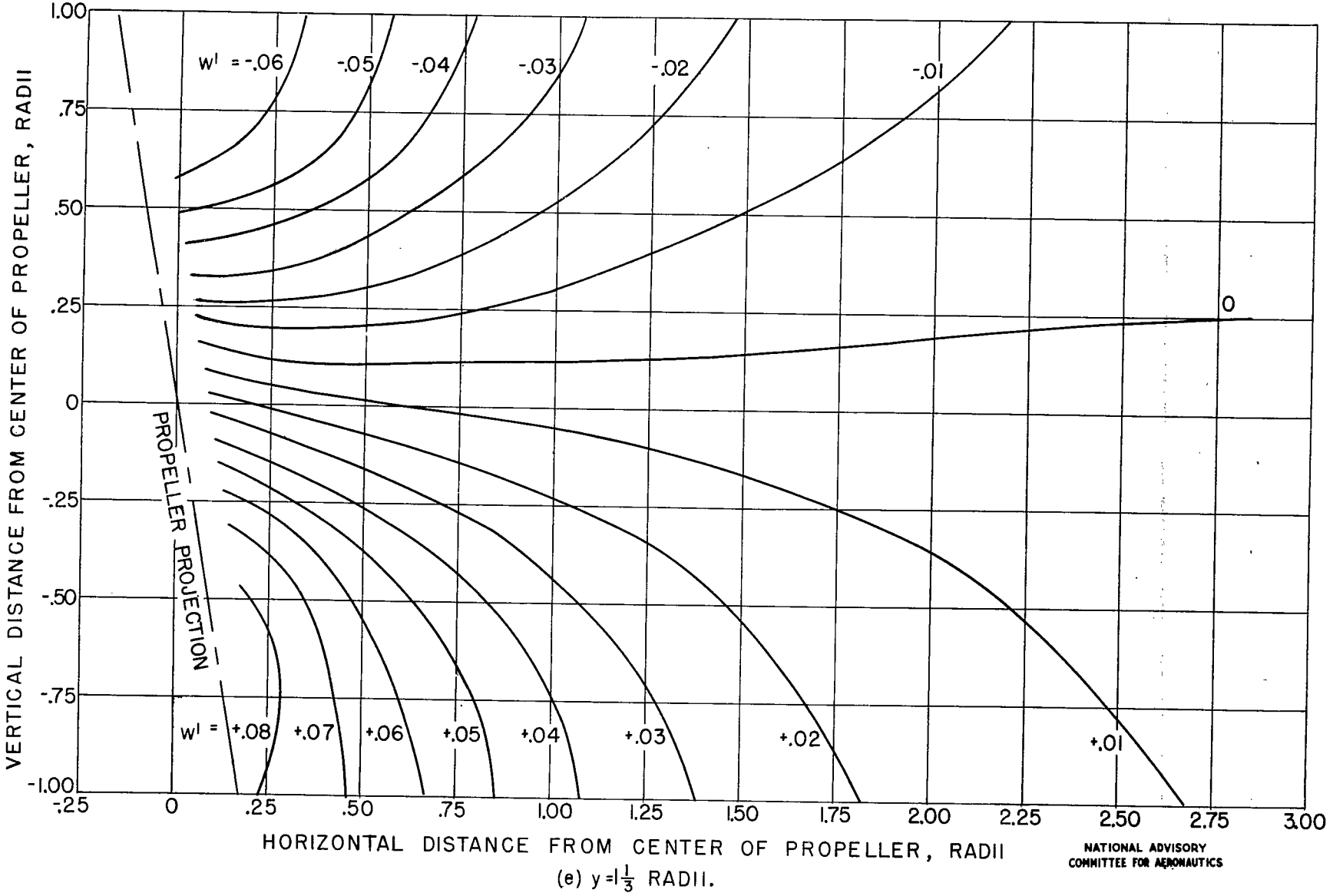

(e) $y = 1\frac{1}{3}$ RADII.

FIGURE 7.- CONTINUED.

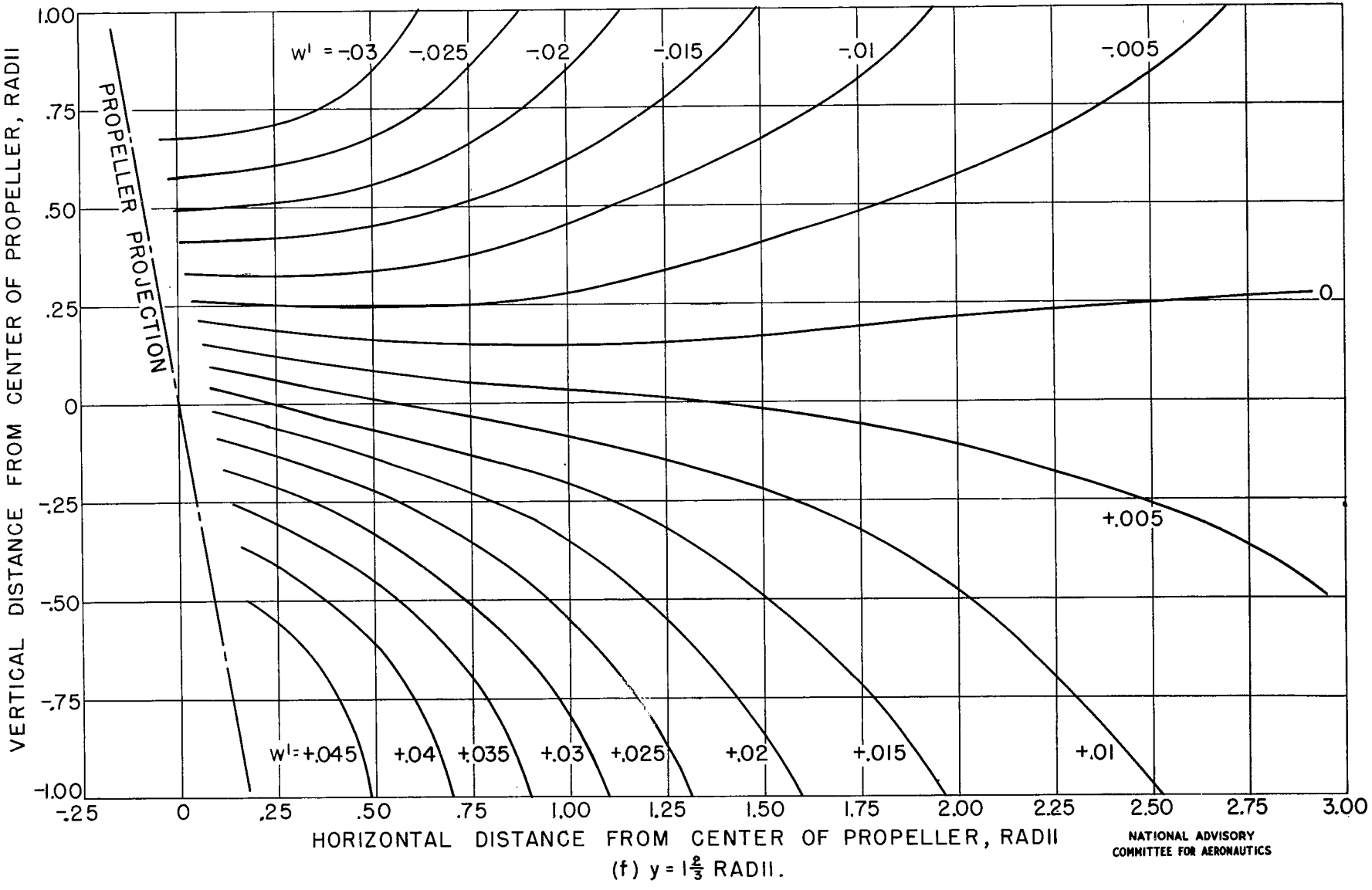

(f) $y = 1\frac{2}{3}$ RADII.

FIGURE 7.- CONTINUED.

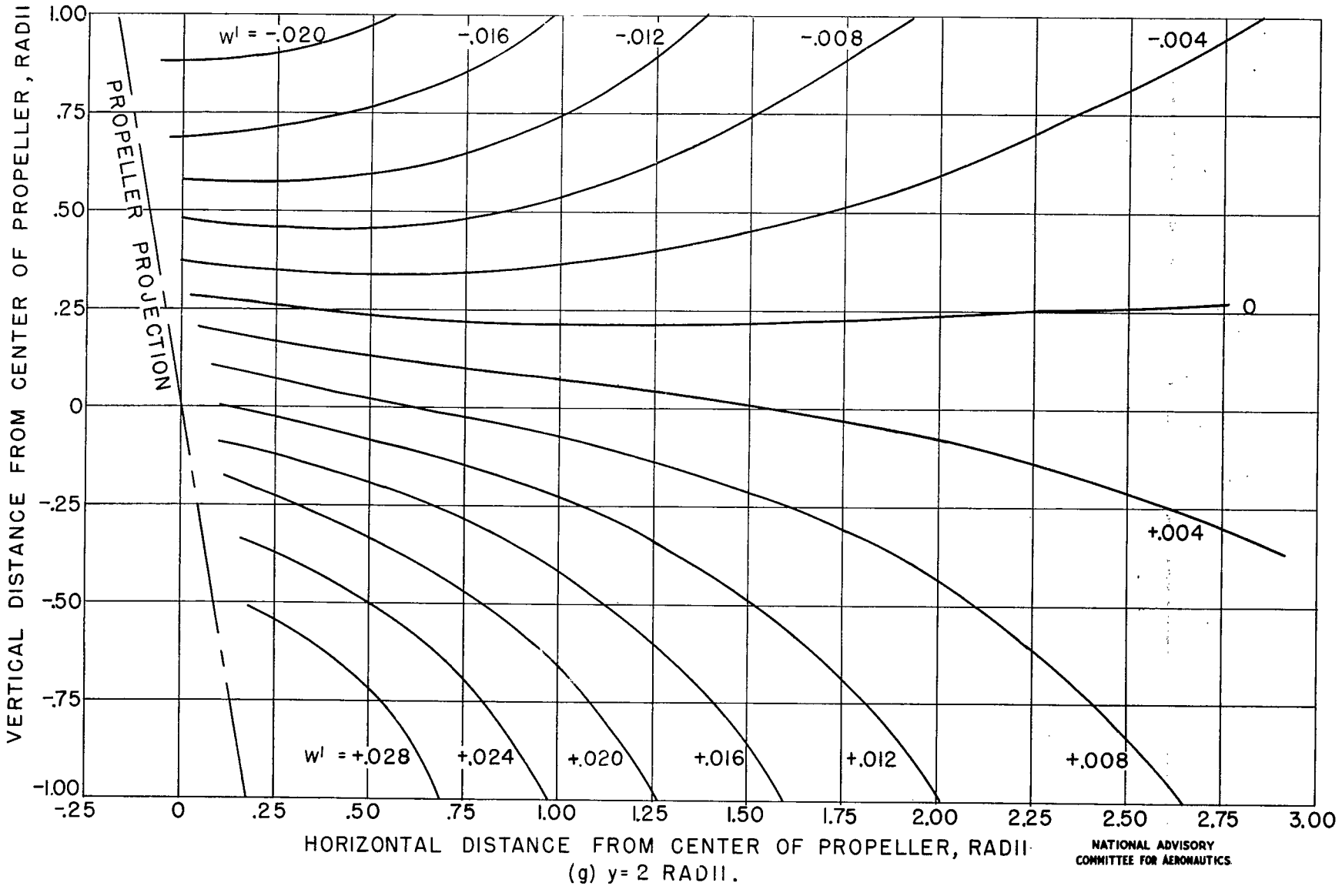

(g) y= 2 RADII.

FIGURE 7.- CONTINUED.

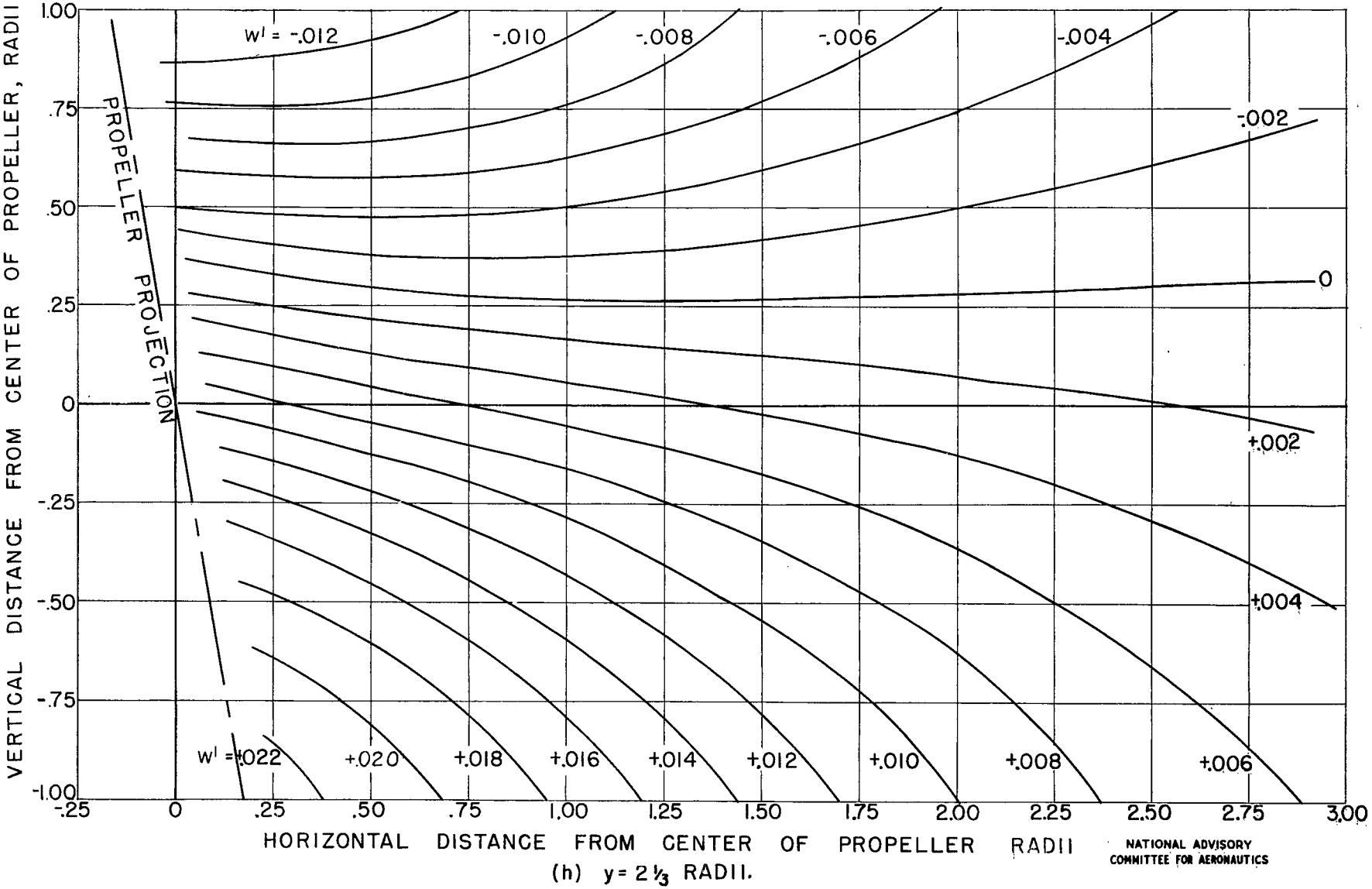

(h) $y = 2\frac{1}{3}$ RADII.

FIGURE 7.- CONTINUED.

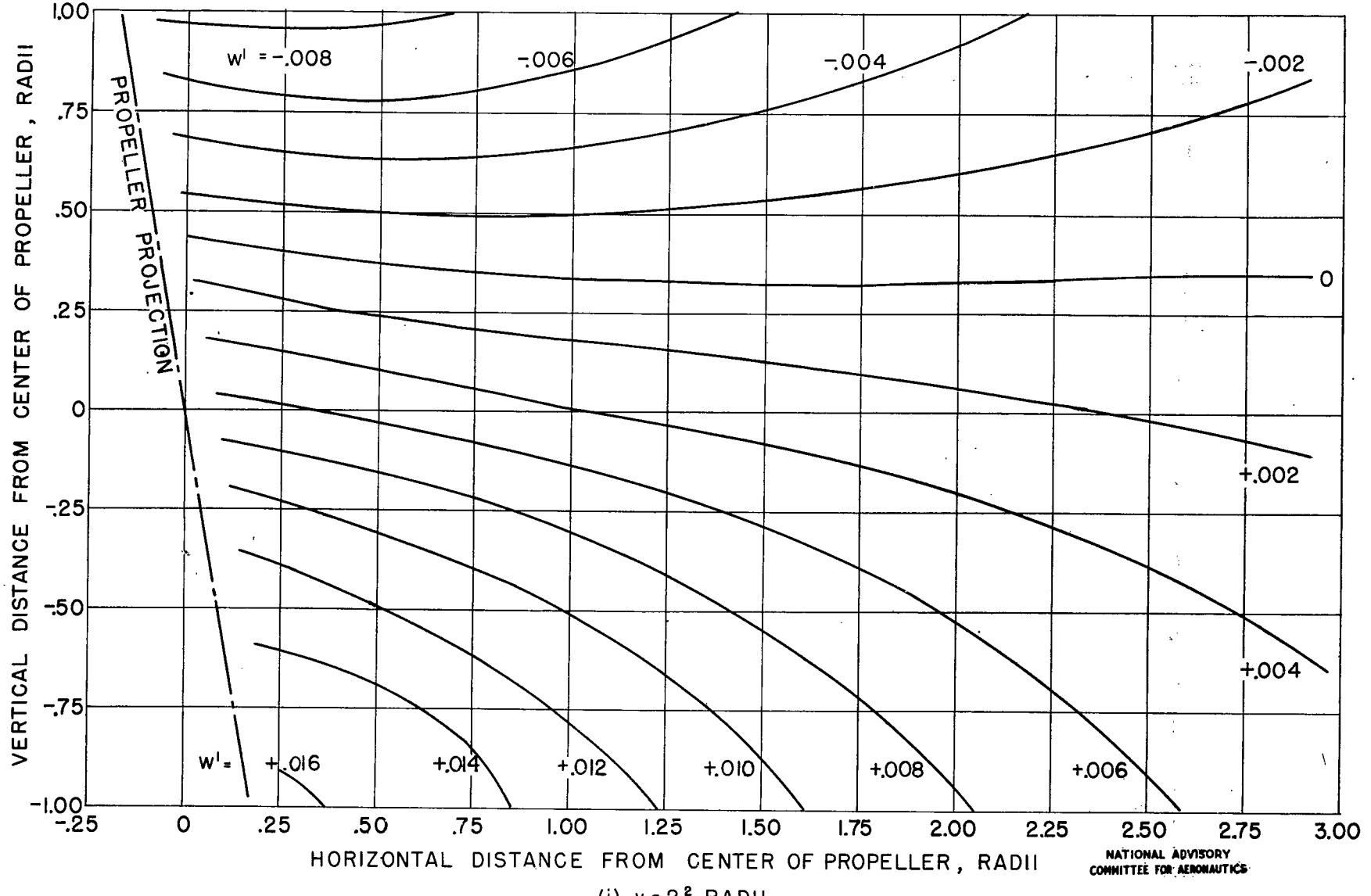

(i) $y = 2\frac{2}{3}$ RADII.

FIGURE 7.- CONCLUDED.

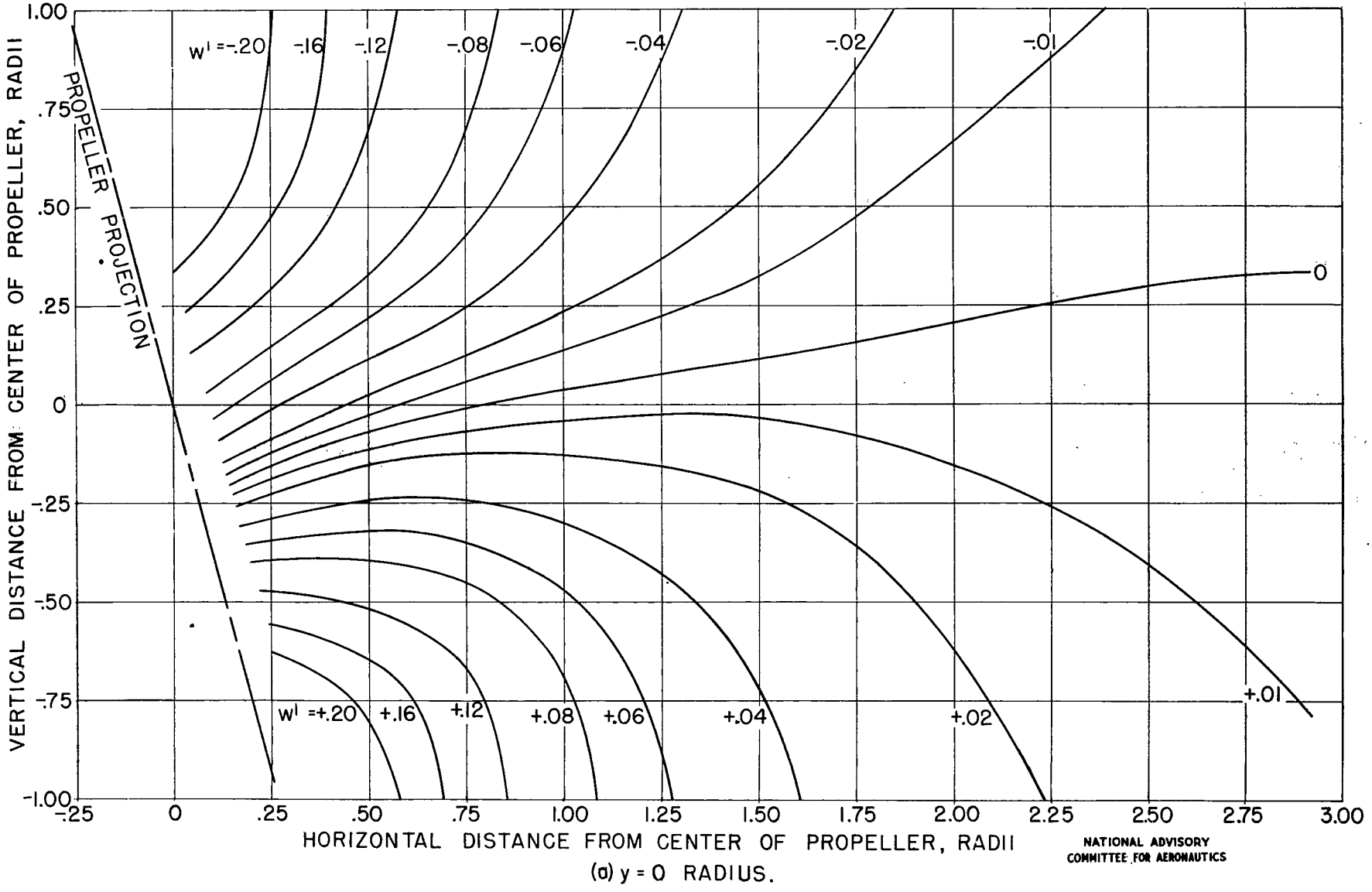

(a) y = 0 RADIUS.

FIGURE 8.- CONTOURS OF CONSTANT VERTICAL VELOCITY FOR $\alpha = 15.°$

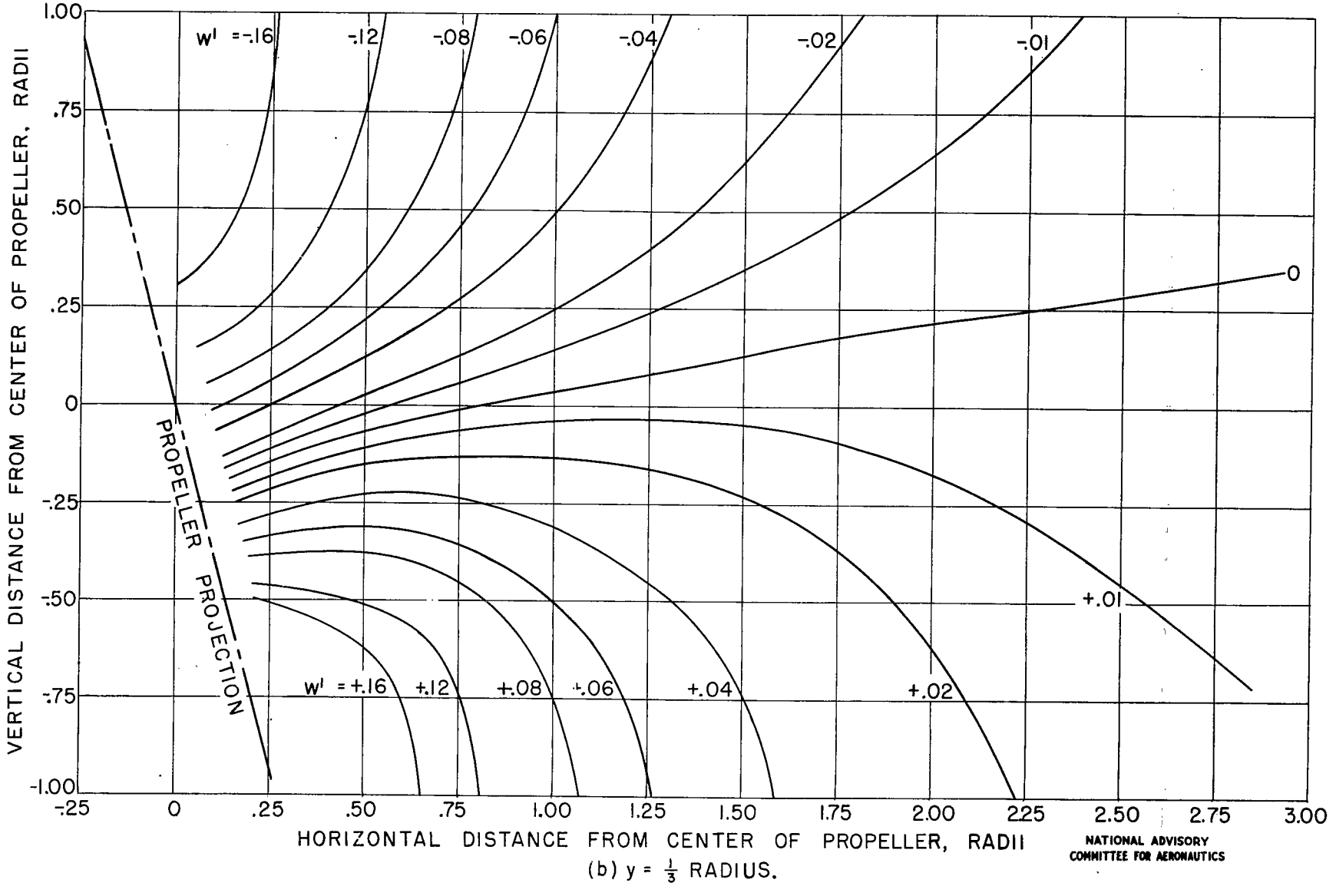

(b) $y = \frac{1}{3}$ RADIUS.

FIGURE 8.- CONTINUED.

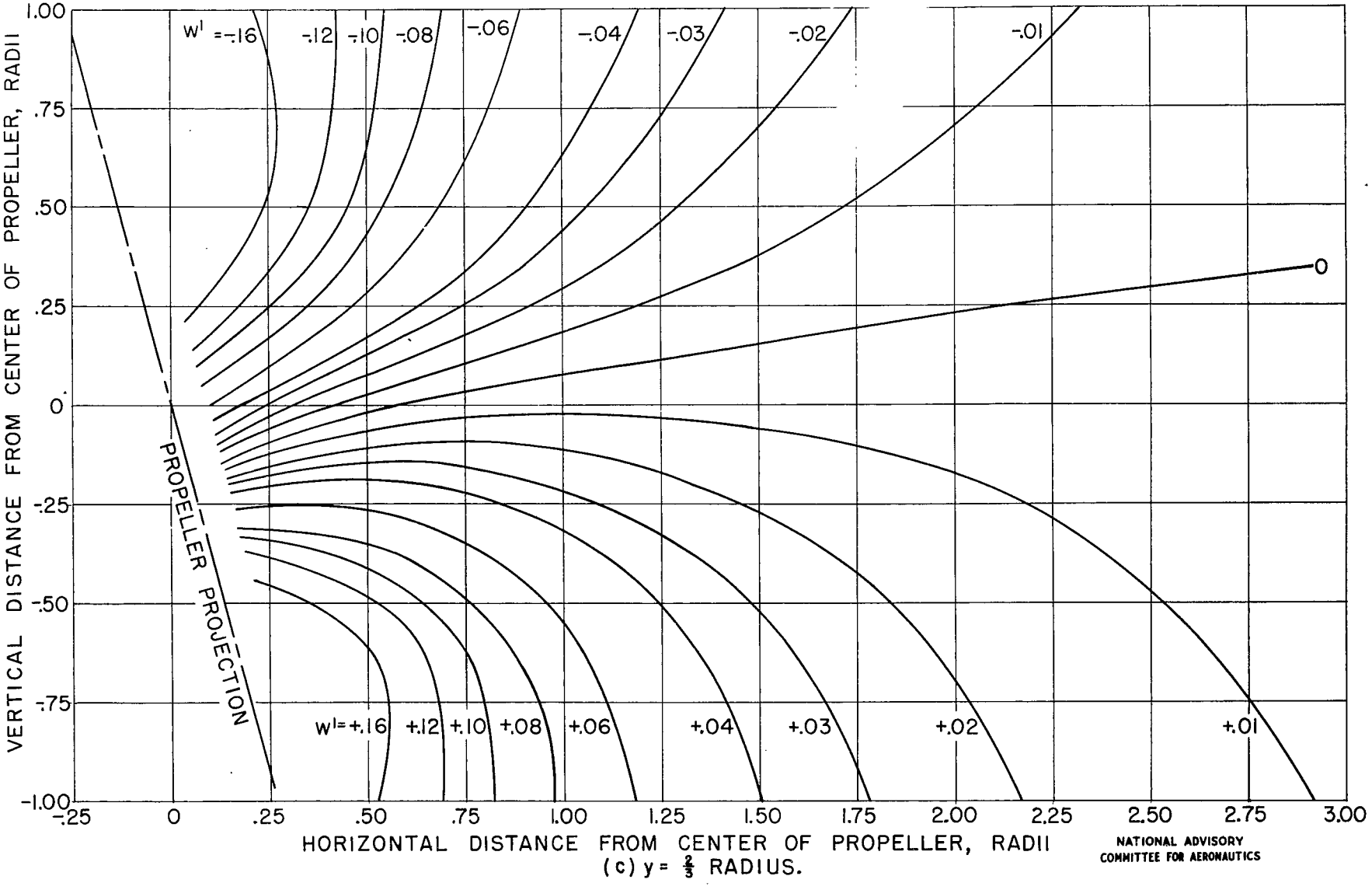

FIGURE 8.- CONTINUED.

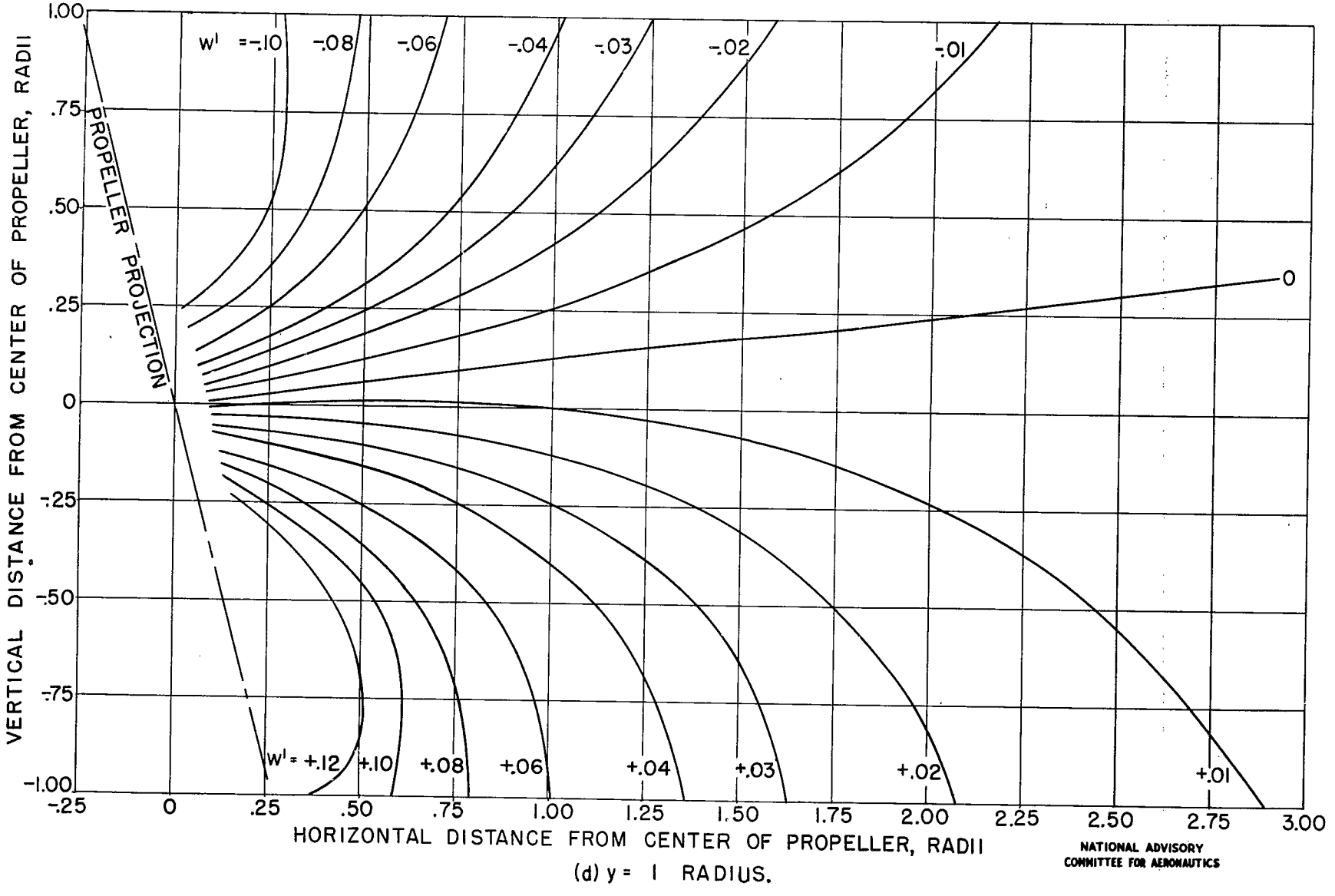

(d) y = 1 RADIUS.

FIGURE 8.- CONTINUED.

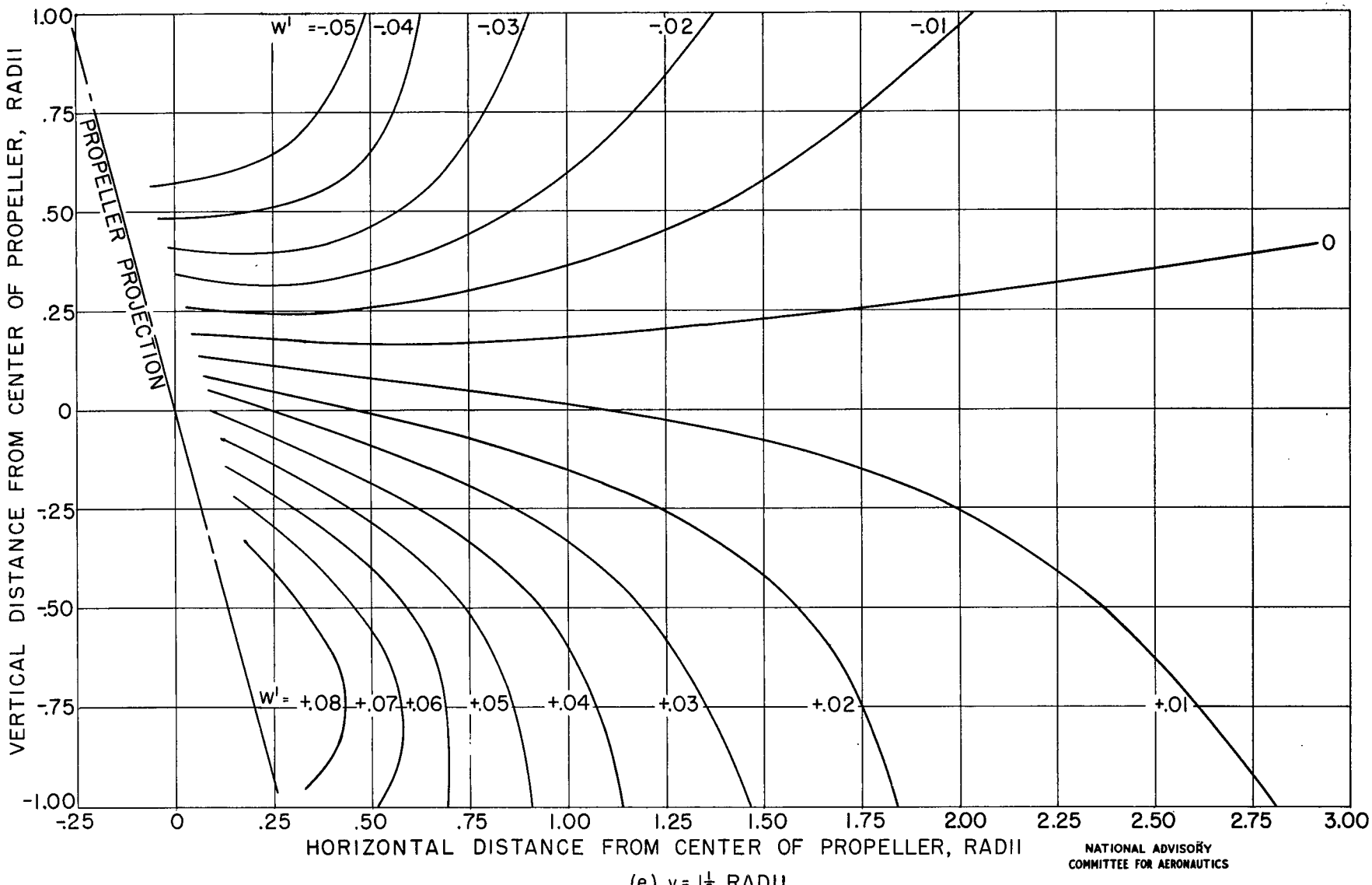

(e) $y = 1\frac{1}{3}$ RADII.

FIGURE 8.- CONTINUED.

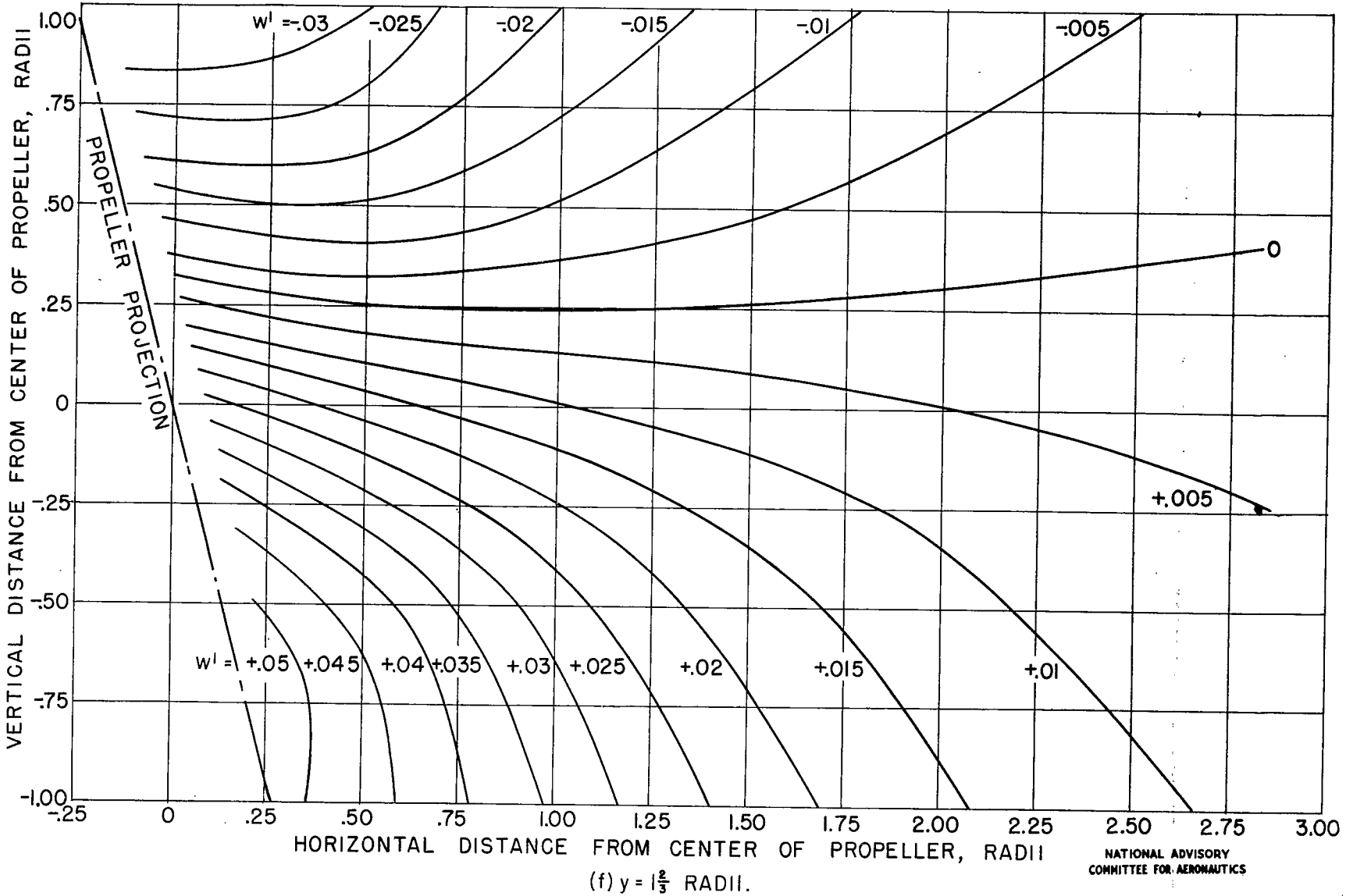

(f) $y = 1\frac{2}{3}$ RADII.

FIGURE 8.- CONTINUED.

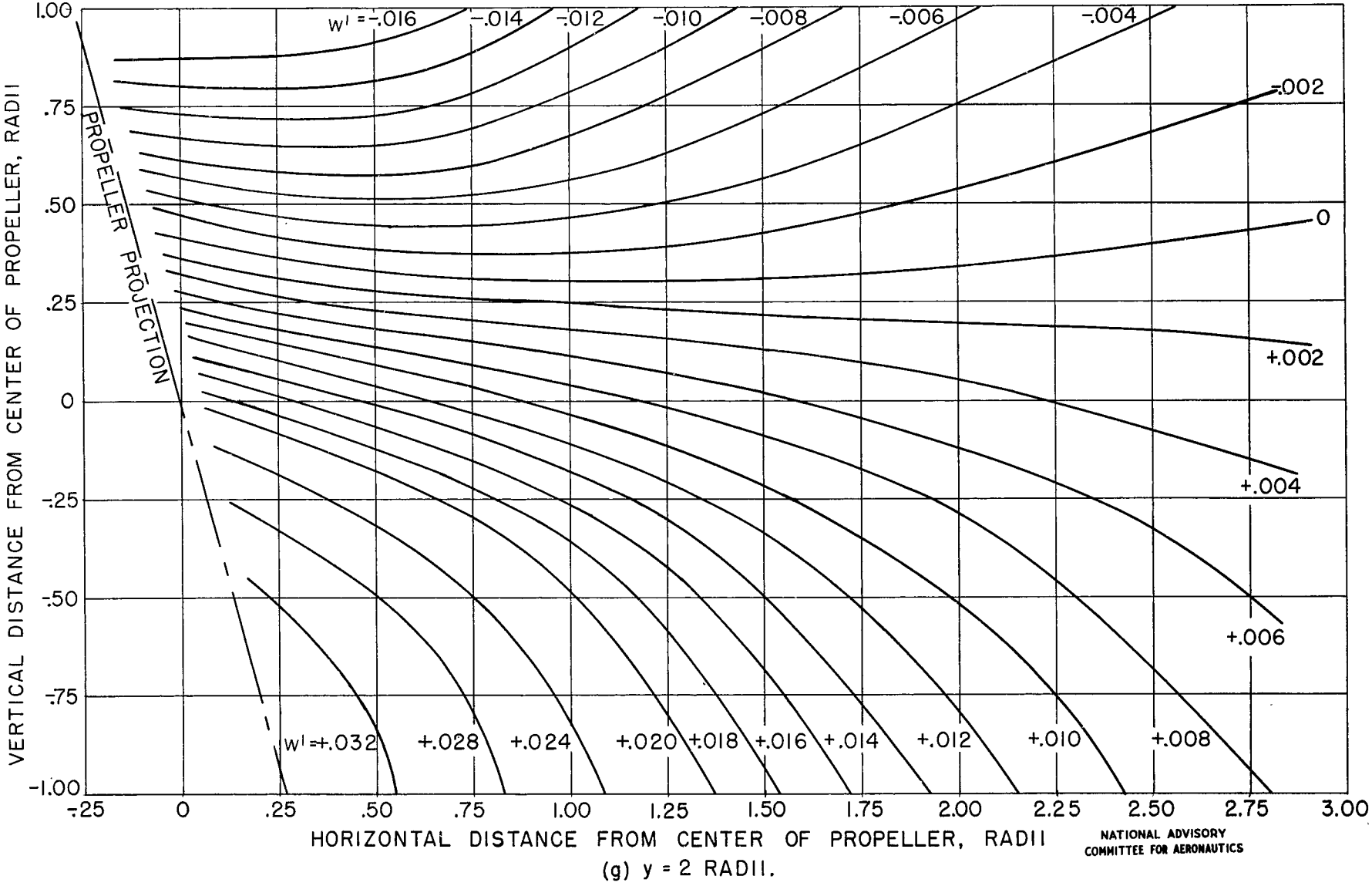

(g) y = 2 RADII.

FIGURE 8.- CONTINUED.

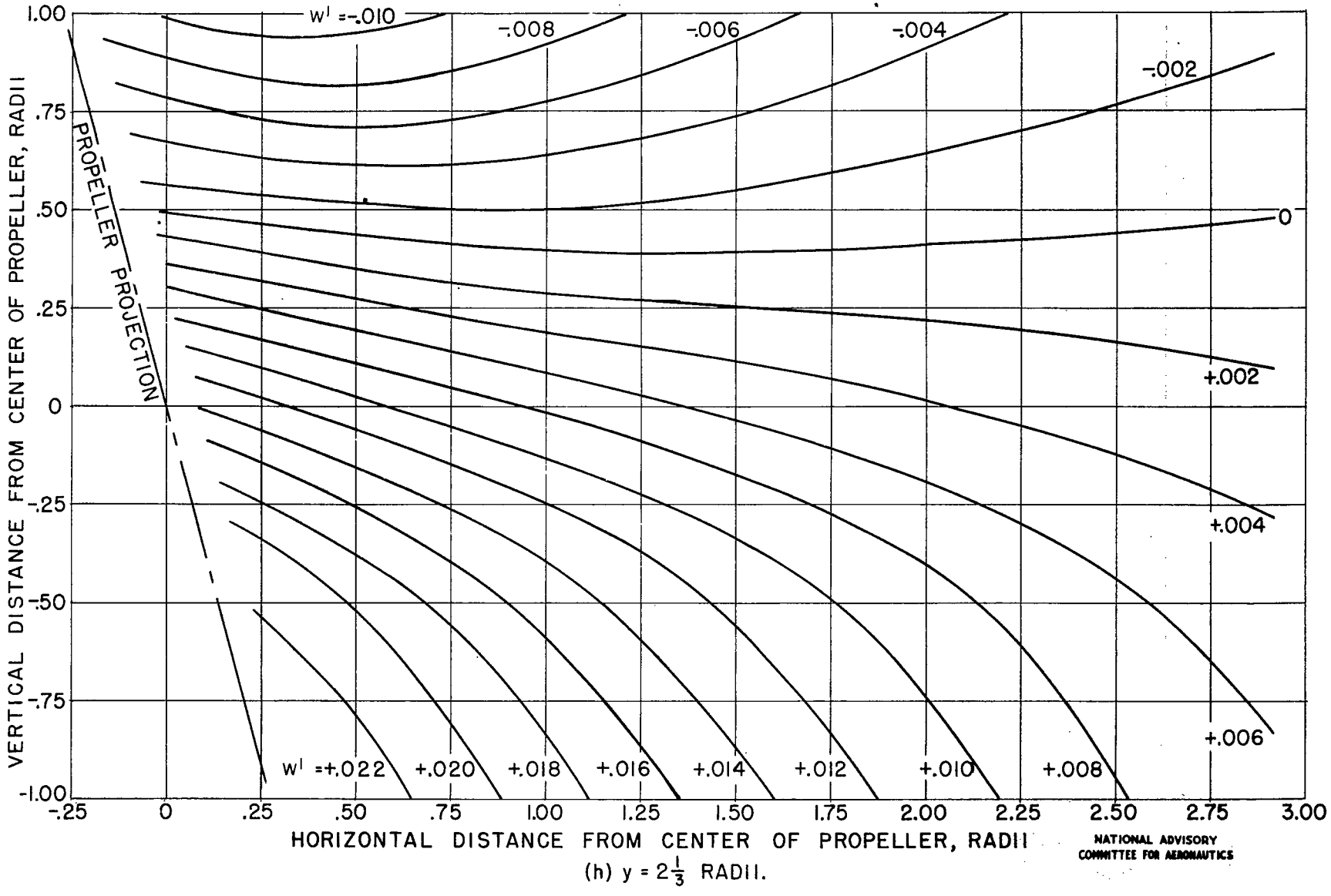

(h) $y = 2\frac{1}{3}$ RADII.

FIGURE 8.- CONTINUED.

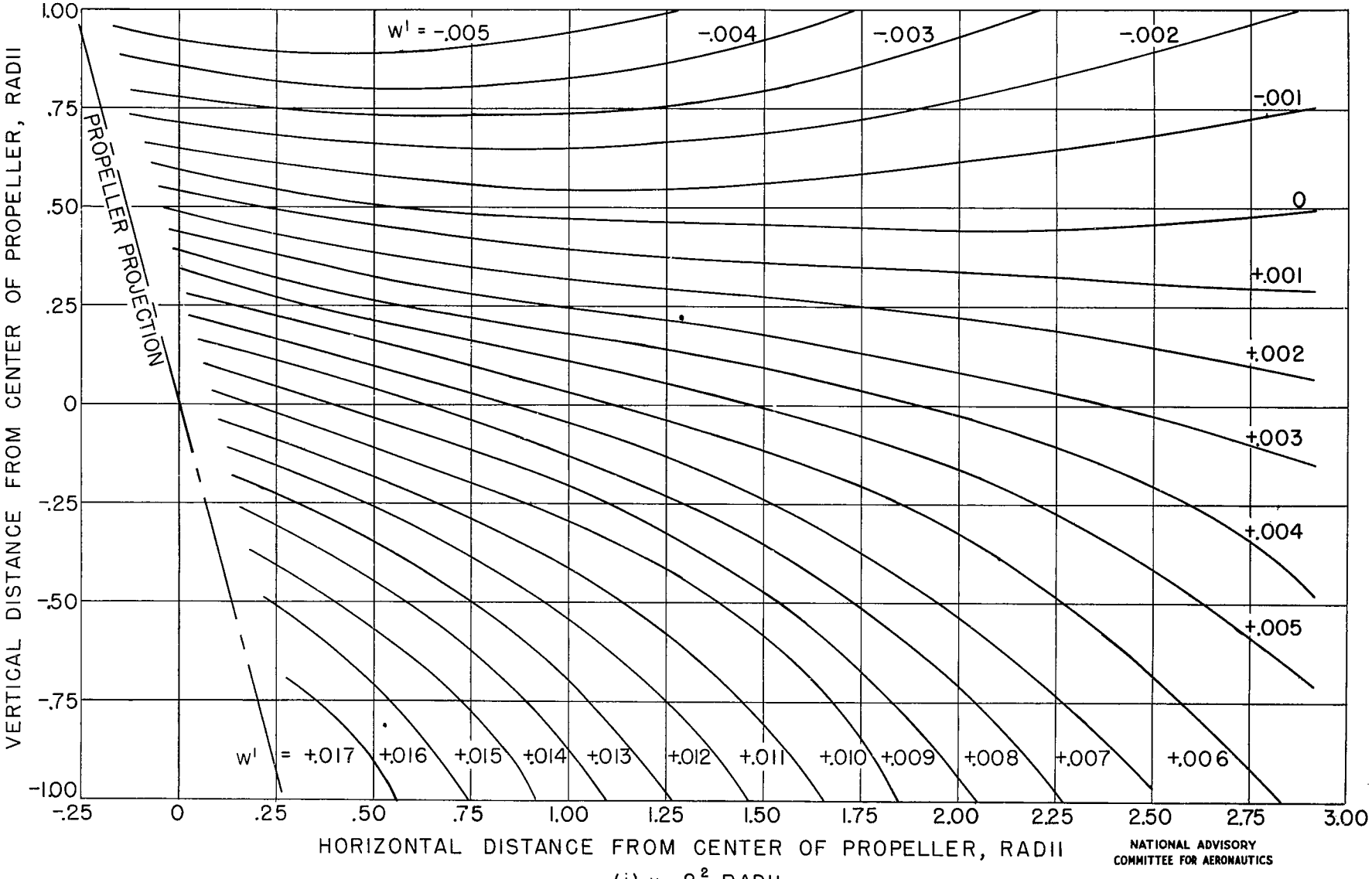

(i) $y = 2\frac{2}{3}$ RADII.

FIGURE 8.- CONCLUDED.

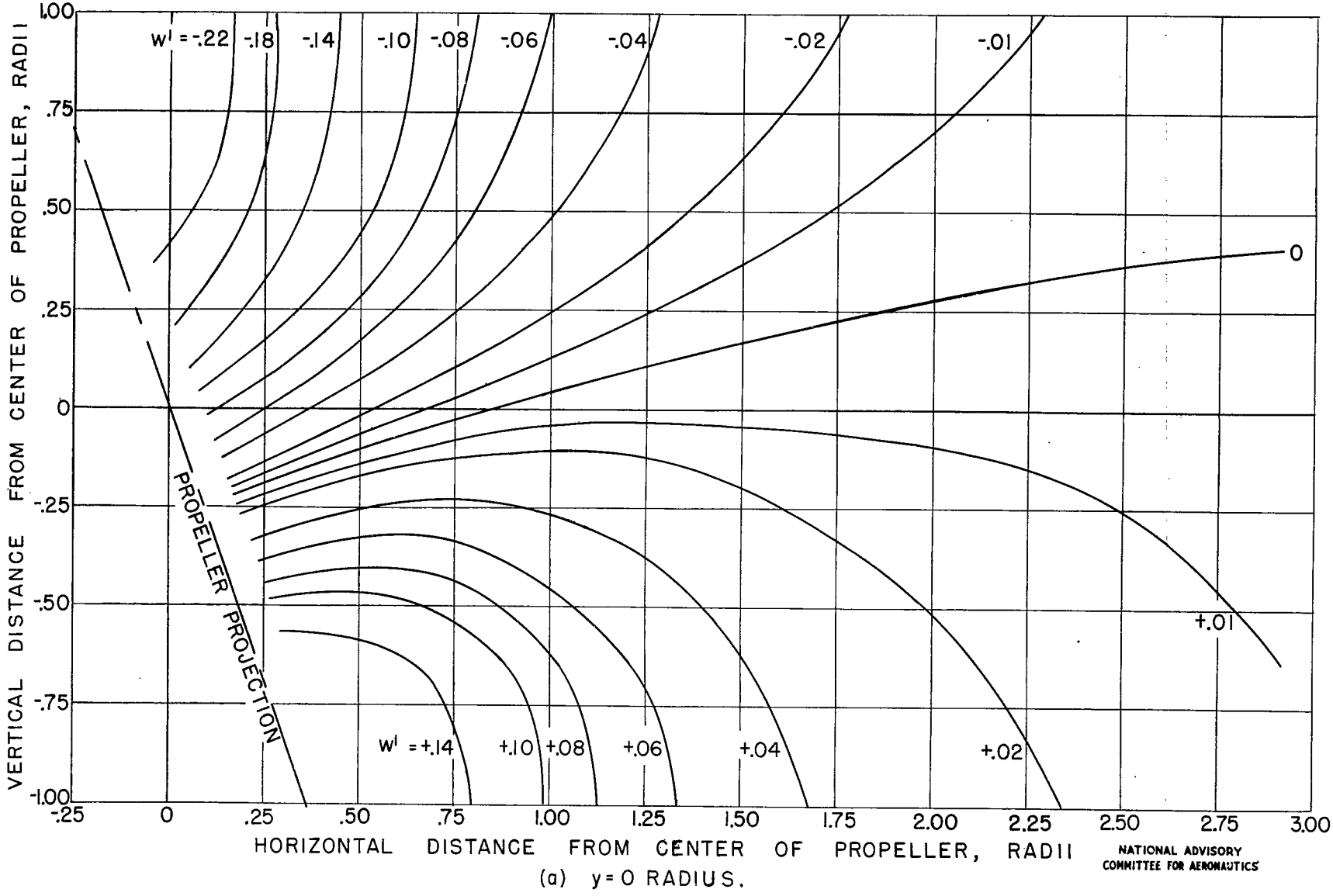

(a) y = 0 RADIUS.

FIGURE 9.- CONTOURS OF CONSTANT VERTICAL VELOCITY FOR $\alpha = 20°$.

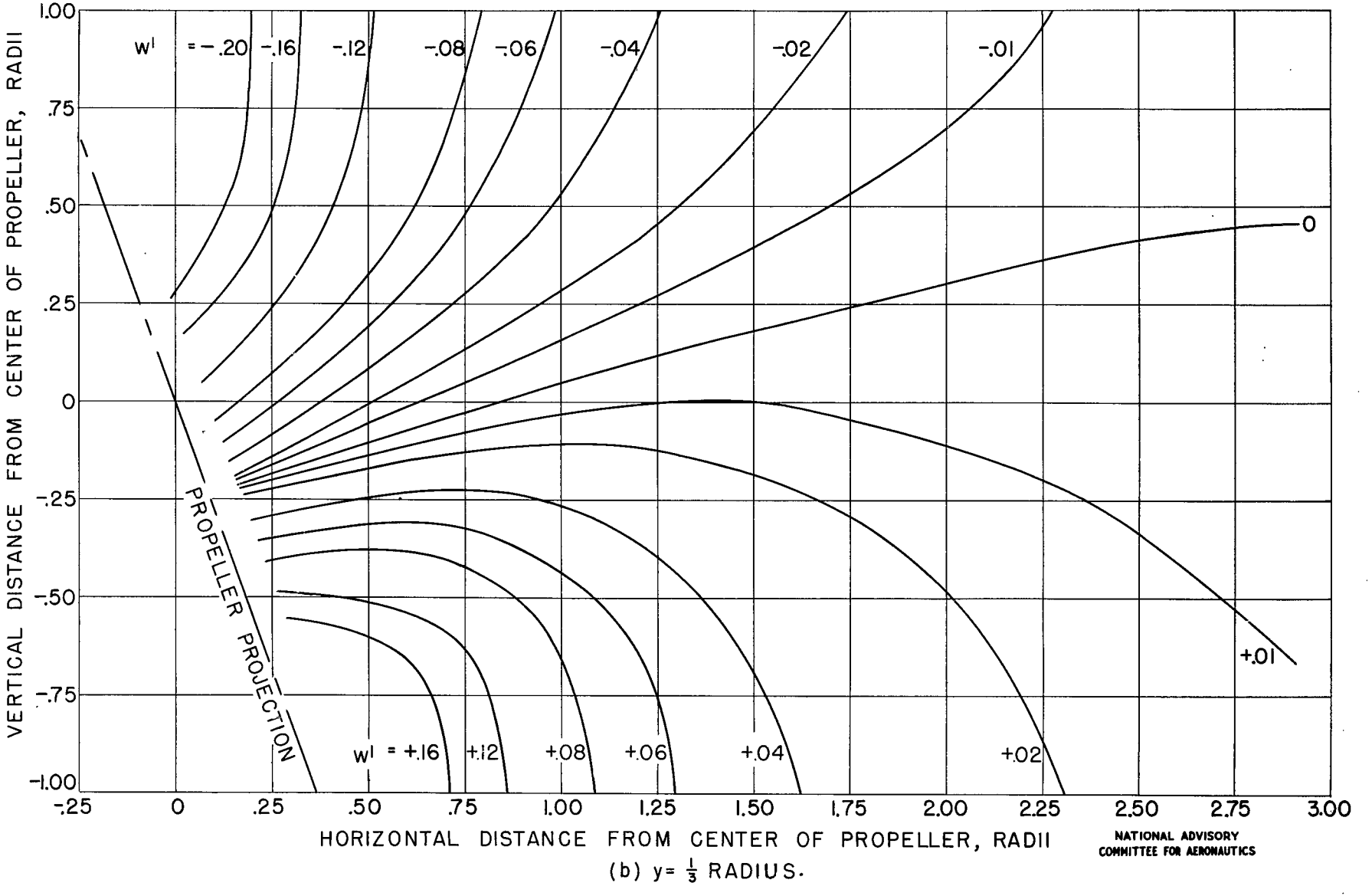

(b) $y = \frac{1}{3}$ RADIUS.

FIGURE 9.- CONTINUED.

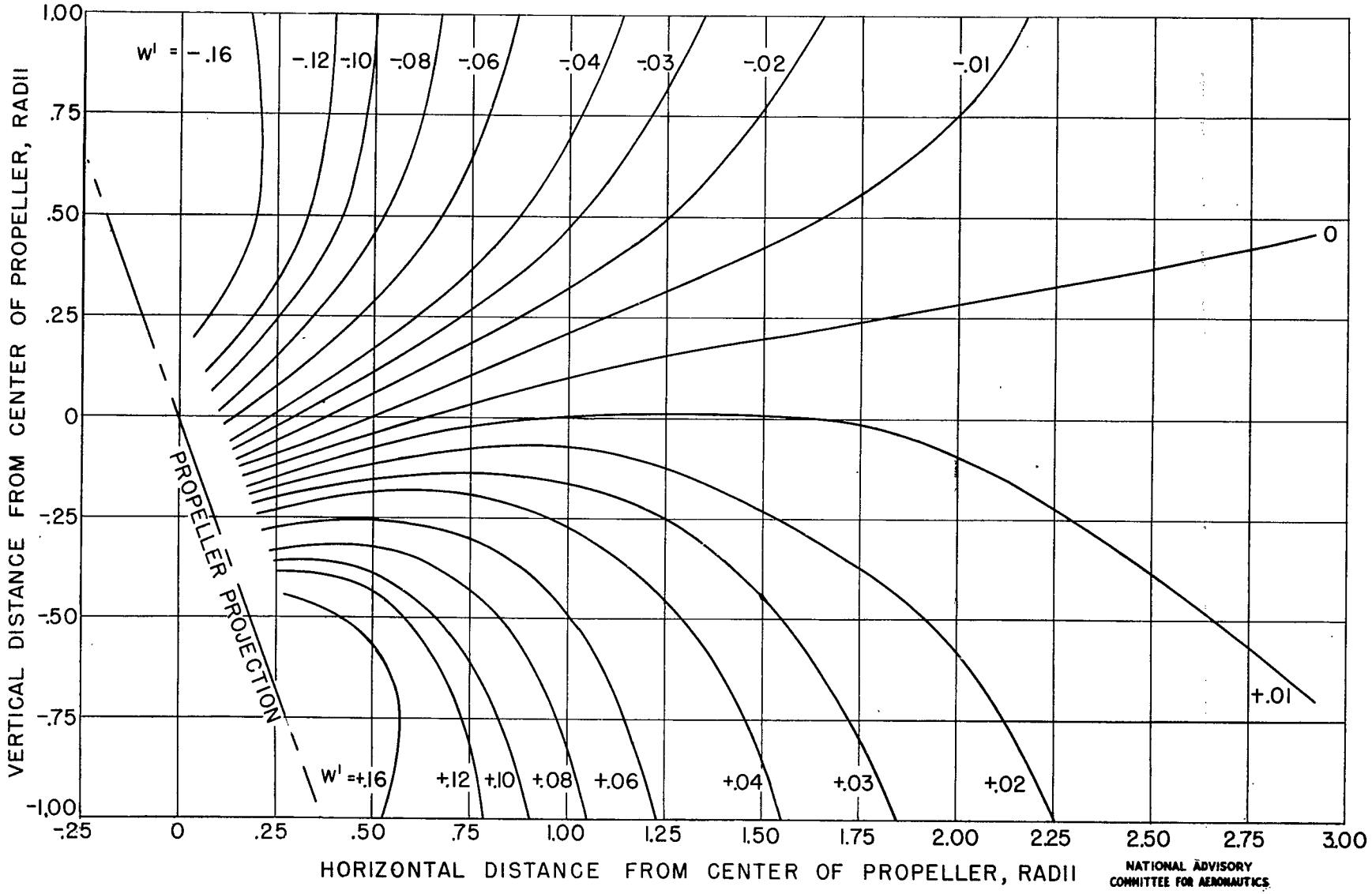

(c) $y = \frac{2}{3}$ RADIUS.

FIGURE 9.- CONTINUED.

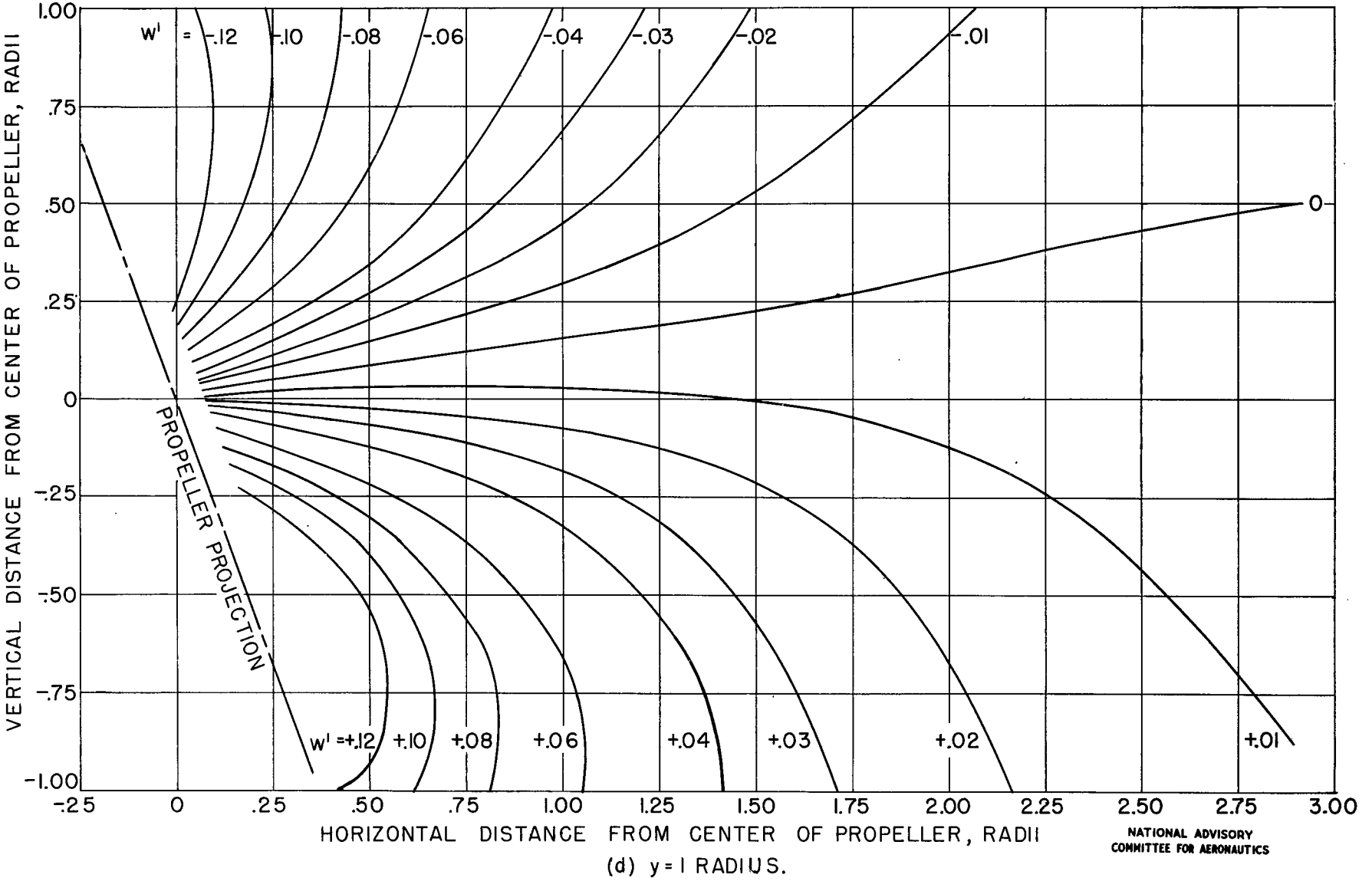

(d) y = 1 RADIUS.

FIGURE 9.- CONTINUED.

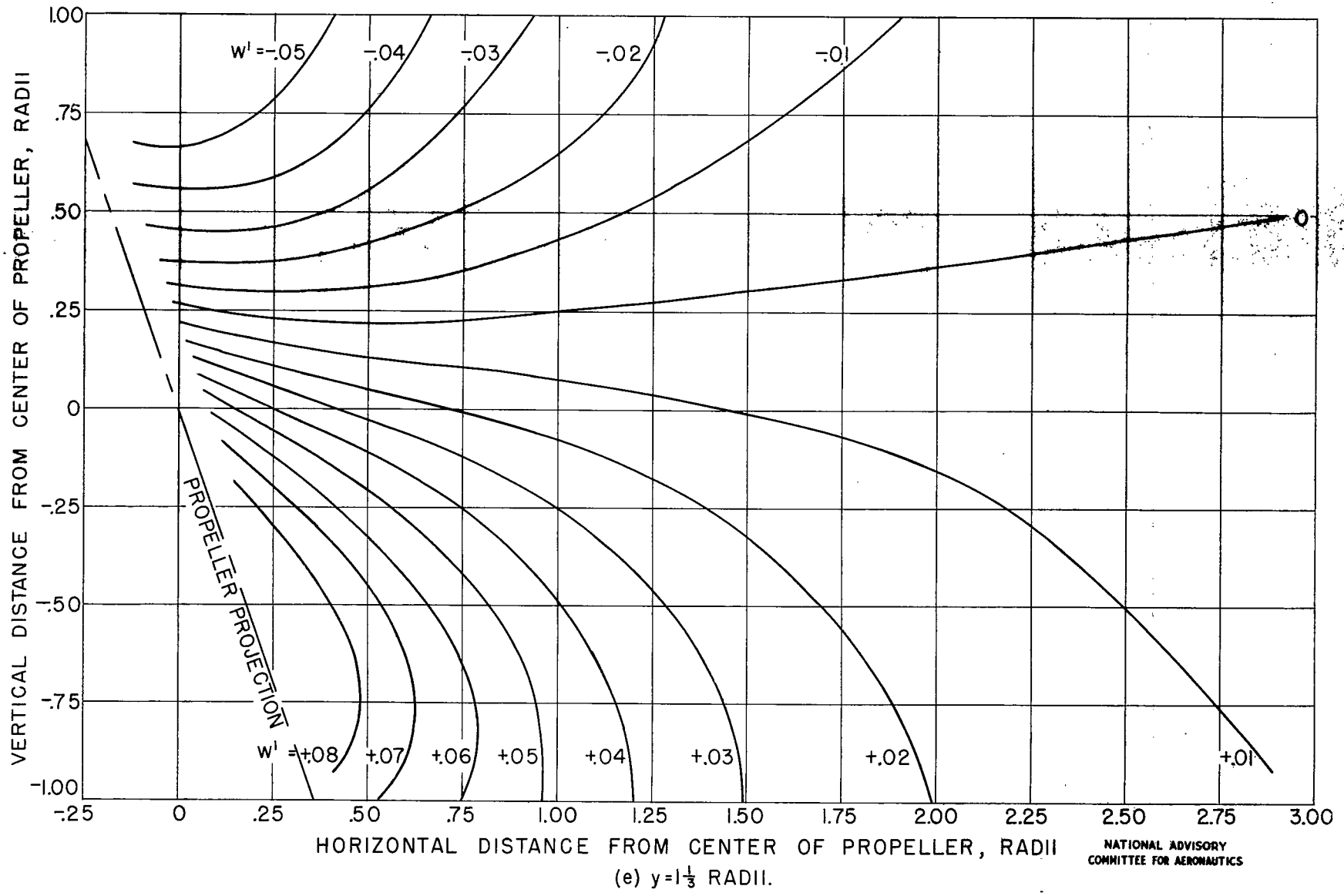

(e) $y = 1\frac{1}{3}$ RADII.

FIGURE 9.- CONTINUED.

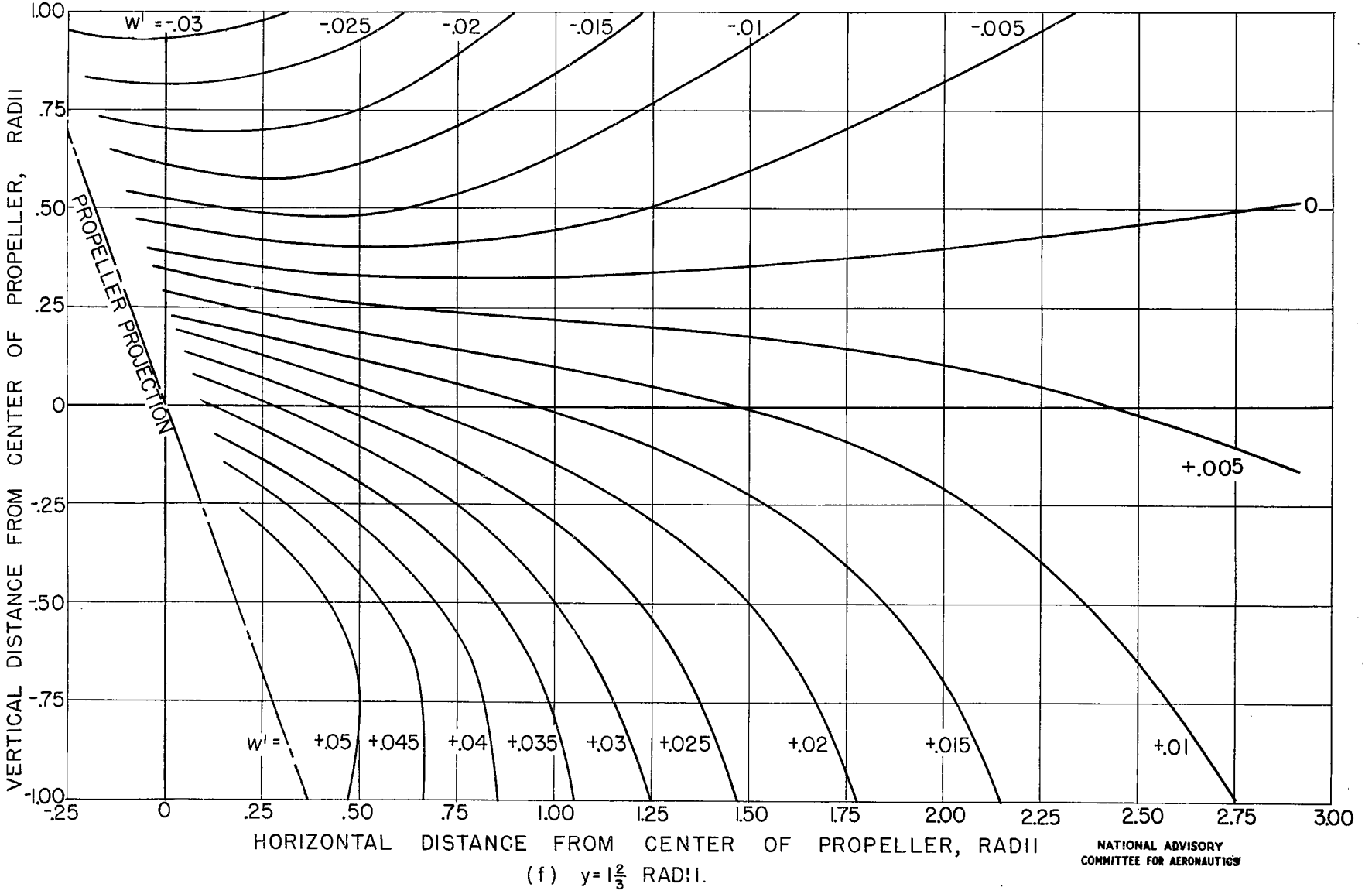

(f) $y = 1\frac{2}{3}$ RADII.

FIGURE 9.- CONTINUED.

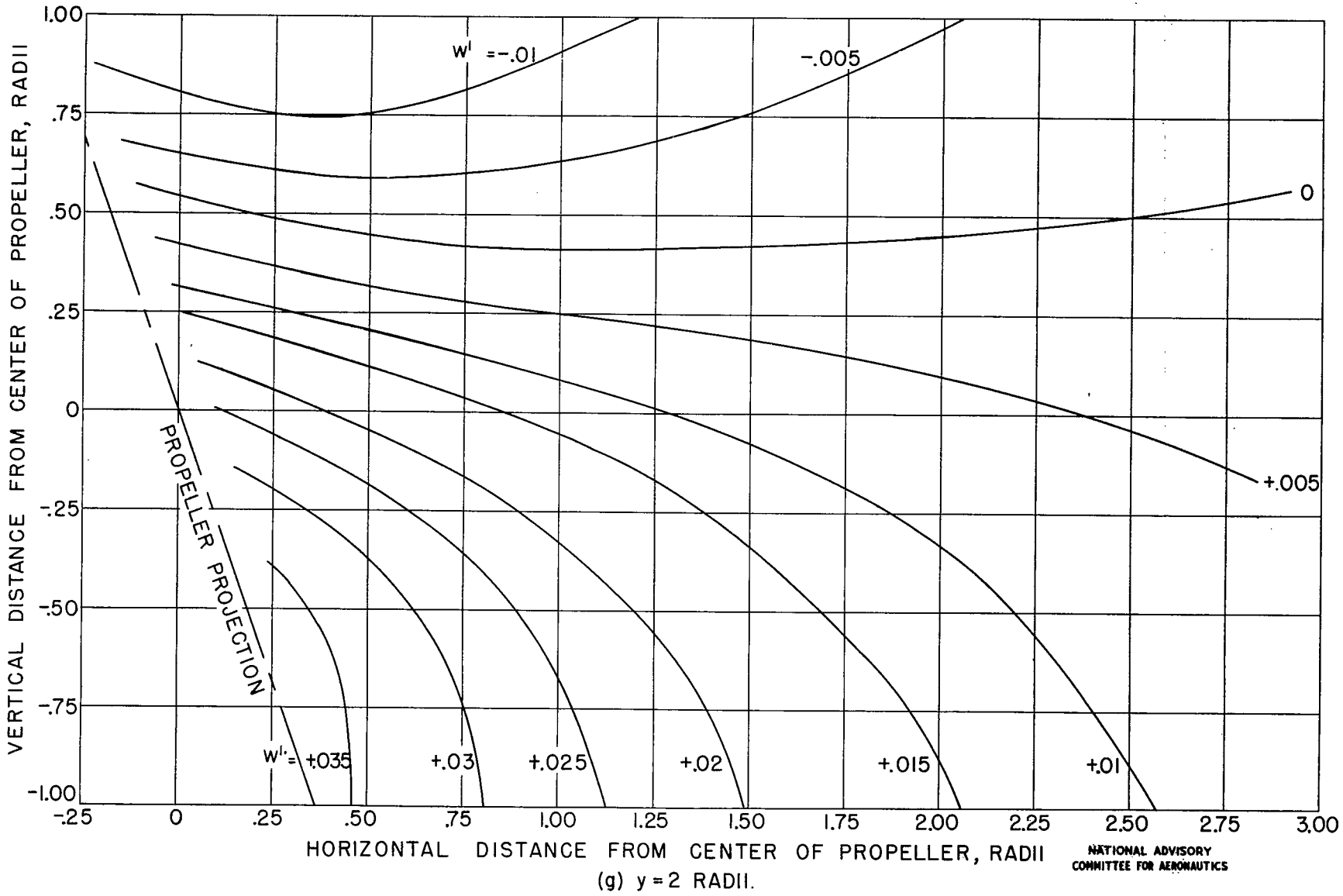

(g) y = 2 RADII.

FIGURE 9.- CONTINUED.

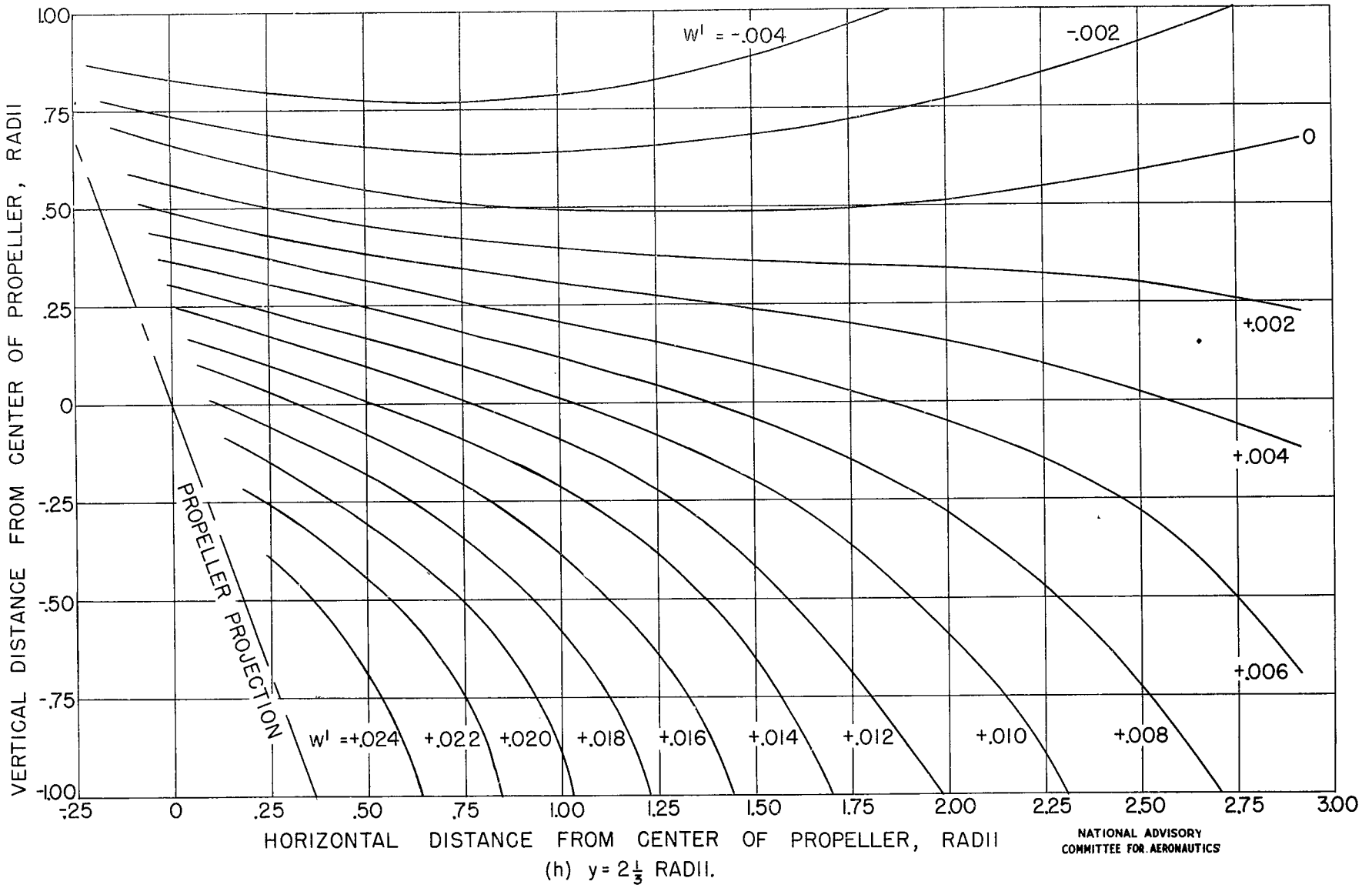

(h) $y = 2\frac{1}{3}$ RADII.

FIGURE 9.- CONTINUED.

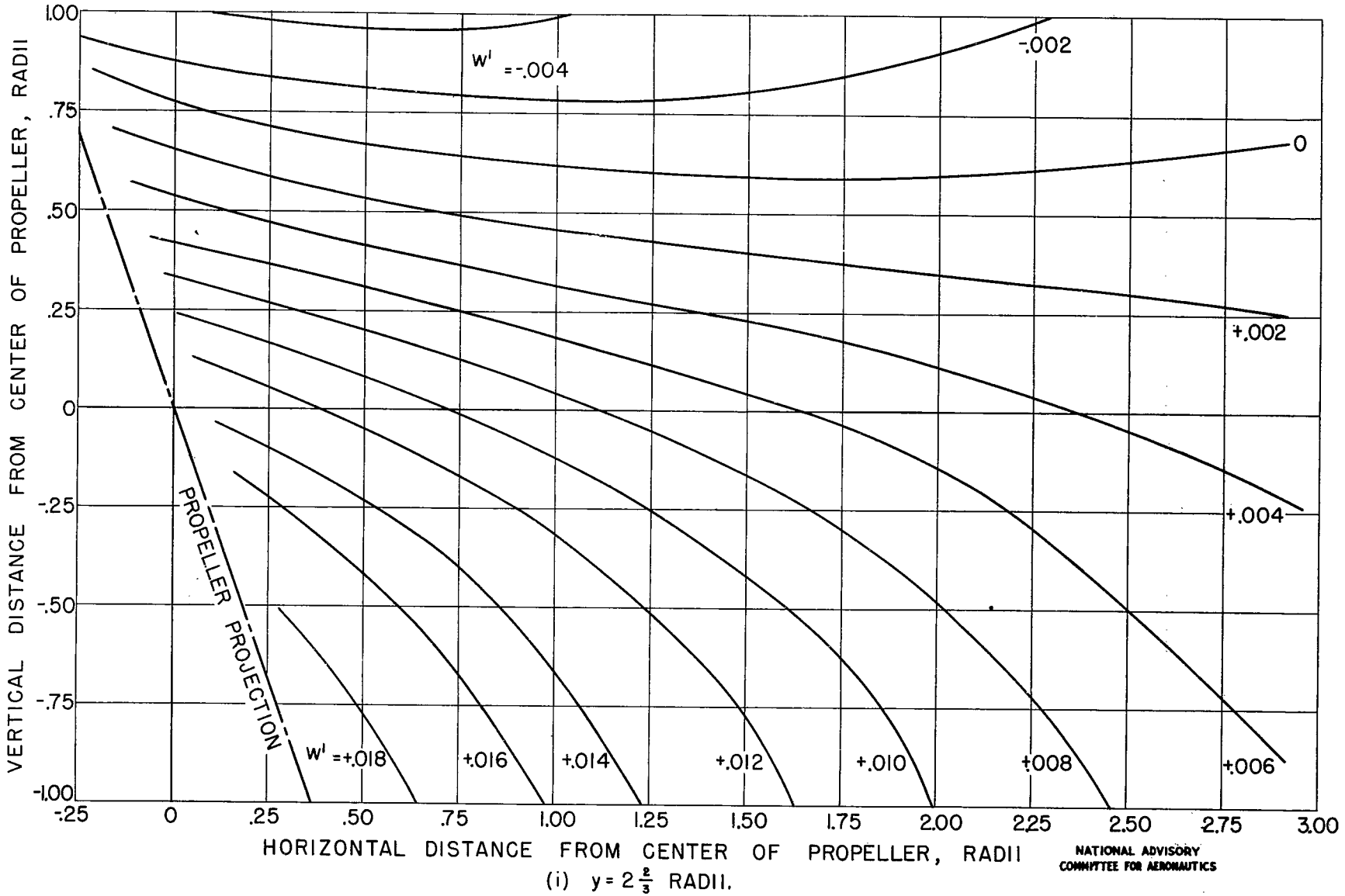

FIGURE 9.- CONCLUDED.

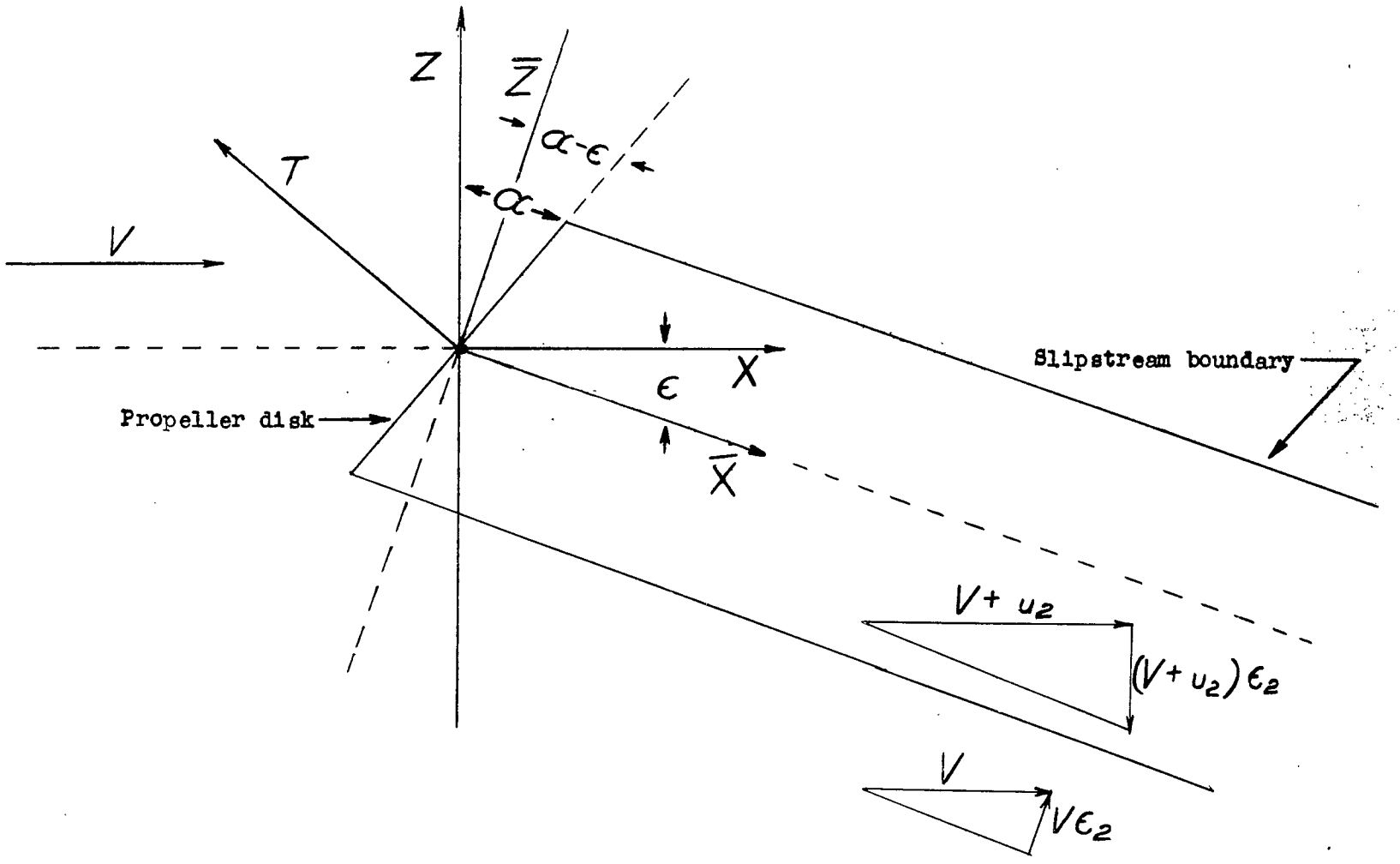

Figure 10.- Downwash behind inclined propeller.

NATIONAL ADVISORY
COMMITTEE FOR AERONAUTICS